Chapter 7
Fundamental Studies on the Electrocatalytic Properties of Metal Macrocyclics and Other Complexes for the Electroreduction of O$_2$

Justus Masa, Kenneth Ozoemena, Wolfgang Schuhmann, and José H. Zagal

Abstract The high prospects of exploiting the oxygen reduction reaction (ORR) for lucrative technologies, for example, in the fuel cells industry, chlor-alkali electrolysis, and metal-air batteries, to name but a few, have prompted enormous research interest in the search for cost-effective and abundant catalysts for the electrocatalytic reduction of oxygen. This chapter describes and discusses the electrocatalysis of oxygen reduction by metallomacrocyclic complexes and the prospect of their potential to be used in fuel cells. Since the main interest of most researchers in this field is to design catalysts which can achieve facile reduction of O$_2$ at a high thermodynamic efficiency, this chapter aims to bring to light the research frontiers uncovering important milestones towards the synthesis and design of promising metallomacrocyclic catalysts which can accomplish the four-electron reduction of O$_2$ at low overpotential and to draw attention to the fundamental requirements for synthesis of improved catalysts. Particular attention has been paid to discussion of the common properties which cut across these complexes and how they may be aptly manipulated for tailored catalyst synthesis. Therefore, besides discussion of the progress attained with regard to synthesis and design of catalysts with high selectivity towards the four-electron reduction of O$_2$, a major part of this chapter highlights quantitative structure–activity relationships (QSAR) which govern the activity and stability of these complexes, which when well understood, refined, and carefully implemented

J. Masa

K. Ozoemena

W. Schuhmann

J.H. Zagal (✉)
Departamento de Química de los Materiales, Facultad de Química y Biología, Universidad de Santiago de Chile, Casilla 40, Correo 33, Santiago, Chile
e-mail: jose.zagal@usach.cl

AU1

should lead to rational design of better catalysts. A brief discussion about nonmacrocyclic copper (I) complexes, particularly Cu(I) phenanthrolines, and those with a laccase-like structure which exhibit promising activity for ORR has been included in a separate section at the end.

7.1 Introduction

Providing adequate, clean, and sustainable energy, from the source of exploitation through eventual disposal, is one of the grand challenges of the twenty-first century. Electrochemical energy storage and conversion systems offer some of the most appealing possibilities for providing clean energy. Of the electrochemical energy systems, fuel cells [1] and metal-air batteries [2] have particularly attracted great research interest. The oxygen reduction reaction (ORR) is one of the key reactions in both of these systems, and Pt is the premium cathode catalyst for the reaction [3]. There is also a growing interest of the importance of ORR in chlor-alkali electrolysis due to its energy saving benefits [4]. Owing to the scarcity of Pt, intensive research has been undertaken aimed at improving both its mass- and area-specific activities through its alloying with less expensive metals and through developments in the synthesis of nanoparticles [5–7]. However, with the awareness that even the most ingenious improvements in catalyst synthesis cannot dispel the issue of Pt scarcity and the potential escalation of its cost upon increased demand, it is a prudent endeavor to explore alternative inexpensive catalysts. Metallomacrocyclic complexes, particularly metalloporphyrins (MPs) and metallophthalocyanines (MPcs), have been widely investigated for ORR since the 1960s [8]. However, due to lack of systematic methodologies for prediction of metallomacrocyclic complexes with satisfactory activity and stability, their performances with regard to both activity and stability generally trail those of catalysts derived from Pt. Of the metallomacrocyclic complexes that have been investigated for ORR, the N_4 metallomacrocyclic complexes, specifically MPs and MPcs, generally exhibit better activity compared to N_2O_2 (Pfeiffer complexes), O_4, N_2S_2, and S_4 macrocyclic chelate complexes [9, 10]. These materials are particularly interesting because of their lower costs compared to noble metals, and their high tolerance to methanol crossover, for the case of methanol fuel cell applications. They are also interesting because they provide models where active centers can be identified, and their catalytic activity can be modulated by changing the structure of the macrocyclic ligand [11]. Several factors influence the activity and stability of metallomacrocyclic complexes for ORR. For a given macrocyclic ligand, ORR will vary with the type of central metal ion [12–15]. Conversely, for a given metal ion, ORR will vary with the nature of substituents on the macrocyclic ligand [16–19], due to the electronic density changes they induce on the metal ion. In addition to these inherent limitations, the ORR activity and stability of a given metallomacrocyclic complex are highly dependent on the pH of the electrolyte. This effect is more pronounced in acidic electrolytes than in alkaline ones [20]. The other factors which
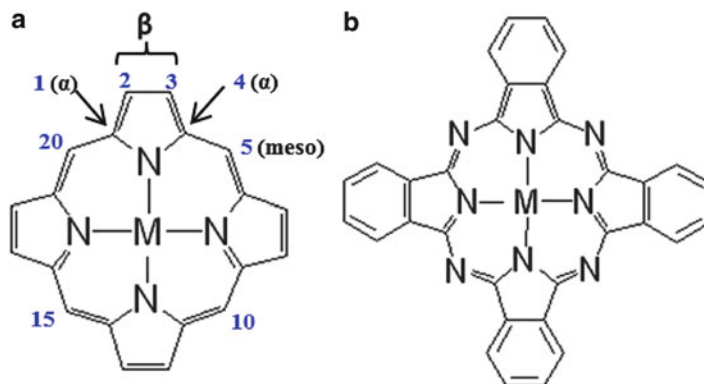
Fig. 7.1 Basic structure of a metalloporphyrin (**a**) and a metallophthalocyanine (**b**)

influence the activity and stability of a given metallomacrocyclic complex include 66
its solubility in a given electrolyte, the method of its immobilization on the 67
electrode, the operating conditions, and whether the ORR is measured with the 68
metallomacrocyclic complex in solution or adsorbed on an electrode [21]. The most 69
commonly used methods for immobilization of metallomacrocyclic complexes on 70
an electrode include dip coating, drop dry, spin coating, electropolymerization, 71
grafting, self-assembled layer(s), sublimation, and spraying. As such, the ORR 72
performance of a given metallomacrocyclic complex may also vary depending on 73
the method of immobilization used. For example, it has been reported in some 74
literature that the potential of the M(III)/M(II) redox couple and oxygen reduction 75
are shifted to more positive values for films formed by electropolymerization 76
compared to films formed by dip coating or drop coating. Therefore, because of 77
the inevitable variations in experimental procedures and conditions from one 78
laboratory to another, it is difficult to make cross-laboratory comparisons of results 79
reported in literature. To avoid delving into this complexity, qualitative and quan- 80
titative structure–activity relationships (QSAR) which govern the activity and 81
stability of metallomacrocyclic complexes have been highlighted, which when 82
well understood, refined, and carefully implemented should form a basis for 83
rational design of improved metallomacrocyclic catalysts for oxygen reduction. 84

MPs and MPcs show very similar physical and chemical properties and they are 85
structurally related to biological catalysts like cytochrome c and hemoglobin. The 86
basic difference between their structures is shown (Fig. 7.1). As it will be discussed 87
in details later, the properties of these complexes are very dependent on the type of 88
central metal (M) and on the nature of substituents on the ligand. It is important to 89
remark that the choice of substituents for the macrocyclic ligands is inexhaustible 90
which leaves plenty of room for tailoring their properties. For example, the 91
properties of metalloporphyrins may be varied widely by means of substitution 92
groups at the β and meso-positions of the ring (Fig. 7.1a). Furthermore, the concepts 93
of supramolecular chemistry and molecular self-assembly offer additional 94
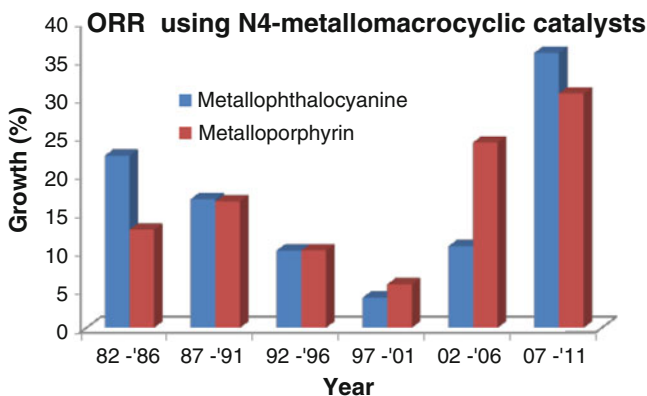possibilities to vary the properties of metallomacrocyclic [22–24]. 95

Fig. 7.2 Graphical representation of the publication growth (% growth = number of publications per 5-year period divided by the total number of publications in the last 30 years, multiplied by 100) from 1982 until 2011. Raw data obtained from SciFinder Scholar(R) search engine

96 Figure 7.2 presents an overview of the intensity of research in the use of MPs and
97 MPcs as electrocatalysts for ORR during the last 4 decades (1982–2011). The graph
98 is interesting as it clearly depicts that intensity of research in ORR follows the
99 trends in global oil prices and world events: increasing as oil prices increase and
100 decreasing as oil prices reduce (see "Oil Price History and Analysis" at http://www.
101 wtrg.com/prices.htm). The 1981/1982 period recorded one of the peak oil prices in
102 history. The increased research interest in ORR using MPs and MPcs in the
103 1982–1986 period may be related to two major events that led to high oil prices:
104 the Iran/Iraq war and the imposition of price controls by the United States on her
105 domestically produced oil, resulting in the US consumers paying more for imports
106 than domestic production.

107 The increased research activity in the 1987–1991 period is associated with the
108 spike in oil prices in 1990 due to low production and the uncertainty relating to
109 invasion of Kuwait by Iraqi and the ensuing Gulf war. Crude oil prices were low
110 over the 1992–1996 period (about US$ 20 per barrel). The 1997–2001 period was
111 the period of the Asian financial crisis that led OPEC to increase oil production
112 quota by 10 %. In fact, this period recorded one of the lowest oil prices in history
113 (about US$ 18 per barrel in 1998). It is not surprising that the intensity of research
114 in ORR for fuel cells and metal-air batteries was at its lowest during this period.
115 Since 2002 to date, research in ORR has continued to increase. This is mostly due to
116 the high oil prices as a result of the Asian economic growth, weak US dollar, Iraq
117 war, world economic recession, and the Arab uprising termed the "Arab spring,"
118 and the increased awareness that the current energy sources cannot fulfill future
119 energy demands. The increased global awareness about the detrimental effects of
120 using fossil energies to the environment and the fact that fossil energy reserves are
121 finite have also in part contributed to the increased intensity of research in ORR for
122 fuel cells.

Apart from high oil prices, the world has increasingly become concerned about the need for environmental protection by minimizing the emission of greenhouse gases emanating from the burning of coal and oil. To address these environmental concerns, most countries of the world are now investing in Research and Development (R&D) for advancement of renewable energy technologies, which may further explain the recent increased research activities in ORR (2002–2011). For example, the USA introduced the Energy Policy Act of 2005 to encourage investment in renewable technologies (http://www.gpo.gov/fdsys/pkg/PLAW-109publ58/pdf/PLAW-109publ58.pdf). In a similar vein, an Advanced Energy Initiative (AEI) related to climate change was introduced in 2006 by the USA to accelerate renewable energy and technologies and reduce greenhouse gas emissions. The AEI provided for a 22 % increase in funding for clean-energy technology research in clean coal technology, nuclear power, and renewable solar and wind energies [25].

7.1.1 Reaction Pathways for the Reduction of Molecular Oxygen

The electrochemical reduction of oxygen in aqueous solutions is a complex multielectron reaction that occurs via two main pathways: one involving the transfer of two electrons to give peroxide and the so-called direct four-electron pathway to give water. The latter involves the rupture of the O–O bond. The nature of the electrode strongly influences the preferred pathway. Most electrode materials catalyze the reaction via two electrons to give peroxide. The several possible pathways are summarized in Table 7.1.

In strongly alkaline solutions or in organic solvents, O_2 is reduced via the transfer of a single electron to give a superoxide ion: $O_2 + e^- \rightleftarrows O_2^-$ ($E^\circ = -0.33$ V vs. NHE). The maximum free energy or the highest oxidant capacity of O_2 is obtained when this molecule reacts on the cathode of a fuel cell via four-electrons. So there is a need for catalysts that promote the four-electron reduction pathway. Most common electrode materials only promote the two-electron pathway, which releases almost one-half the free energy compared to that of the four-electron pathway. This is due in part to the relatively high dissociation energy of the O–O bond (118 kcal/mol). The four-electron reduction of O_2 to give water involves the rupture of the O–O bond and can involve the interaction of O_2 with one site (single site) or with two active sites simultaneously (dual site) on the electrode surface (Fig. 7.3).

Upon these possible interactions, the energy of the O–O bond decreases, favoring its rupture since electrons accepted by the O_2 molecule will occupy antibonding π^* orbitals. On platinum, O_2 reduction occurs almost entirely via four-electrons [26]. It is likely that on this metal O_2 interacts via the "bridge *cis*" conformation, involving two metal active sites (see Fig. 7.3) since the Pt–Pt separation in certain crystallographic orientations is optimal for this type of interaction. It is then crucial

Table 7.1 Possible pathways for the oxygen reduction in aqueous media

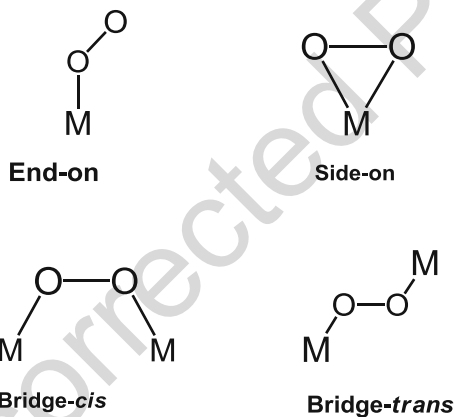| Mode of interaction	ORR pathways	
	Acidic medium	Basic medium
Bridge (or) trans	$O_2 + 2e^- + 2H^+ \rightarrow 2OH_{ads}$	$O_2 + 2e^- + 2H_2O \rightarrow 2OH_{ads} + 2OH^-$
	$2OH_{ads} + 2H^+ + 2e^- \rightarrow 2H_2O$	$2OH_{ads} + 2e^- \rightarrow 2OH^-$
	Overall direct reaction	Overall direct reaction
	$O_2 + 4H^+ + 4e^- \rightarrow 2H_2O$	$O_2 + 2H_2O + 4e^- \rightarrow 4OH^-$
	$E^o = 1.23\ V_{NHE}$	$E^o = 0.401\ V_{NHE}$
End-on	$O_2 + e^- + H^+ \rightarrow HO_{2,ads}$	$O_2 + H_2O + e^- \rightarrow HO_{2,ads} + OH^-$
	$HO_{2,ads} + e^- + H^+ \rightarrow H_2O$	$HO_{2,ads} + e^- \rightarrow HO_2^{\bullet}$
	Overall indirect reaction	Overall indirect reaction
	$O_2 + 2e^- + 2H^+ \rightarrow H_2O_2$	$O_2 + H_2O + 2e^- \rightarrow HO_2^{\bullet} + OH^-$
	$E^o = 0.682\ V_{NHE}$	$E^o = -0.076\ V_{NHE}$
	with $H_2O_2 + 2H^+ + 2e^- \rightarrow\ 2H_2O$	with $HO_2^{\bullet} + H_2O + 2e^- \rightarrow 3OH^-$
	$E^o = 1.77\ V_{NHE}$	$E^o = 0.88\ V_{NHE}$

Fig. 7.3 Different spatial configurations for molecular oxygen when it interacts with metal sites

to develop low-cost catalysts that decrease the overpotential of the reduction of O_2 and that can also promote the four-electron reduction.

7.1.2 Evaluation of Catalysts for ORR

It is desirable to evaluate potential catalysts for fuel cell reactions in fuel cell prototypes under the real conditions of application. The standard approach involves profiling the voltage and power output as a function of the current drawn by a load during operation of a fuel cell. A schematic representation of the typical features of the voltage/power–current graphs is shown in Fig. 7.4. Fuel cells generally exhibit a

Fig. 7.4 Schematic representation of the typical voltage/power–current curves during operation of a fuel cell
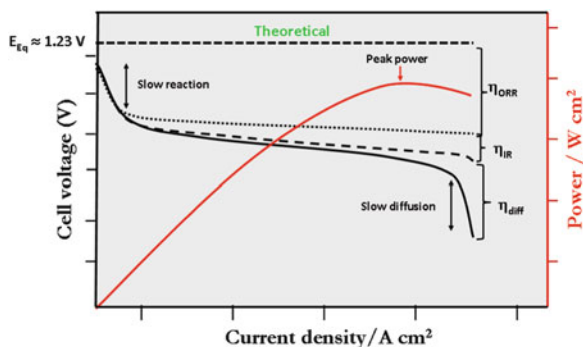
substantial drop in voltage from the theoretically expected maximum voltage, even 171
at their open circuit potential. When a load is applied to the cell, the cell voltage 172
drops further as more and more current is drawn from it. For intermediate current 173
densities, the voltage drops linearly as the current drawn from it is increased as 174
shown in Fig. 7.4. As the current drawn from the cell is increased further up to some 175
point, mass-transport limitation of either reactants, products, or both ensues and a 176
drastic decline in the cell voltage is observed. 177

The effective voltage E of a fuel cell at a given current density, taking into 178
account the various voltage loses, is given by $E = E_{eq} - \eta_{ORR} - \eta_{IR} - \eta_{diff}$, where 179
E_{eq} is the theoretical thermodynamic voltage, η_{ORR} is the activation overpotential 180
due to slow electrode reactions, η_{IR} is the overpotential due to ohmic resistances in 181
the cell, and η_{diff} is the overpotential due to slow diffusion of reactants, products, or 182
both. For hydrogen fuel cells, the voltage losses due to electrooxidation of H_2 at the 183
anode are insignificant compared to the voltage losses due to ORR. Therefore, when 184
comparing different catalysts for a given fuel cell configuration, the best catalyst or 185
pair of catalysts for the anodic and cathodic reactions should be the one(s) which 186
exhibit(s) minimum loss in cell voltage at a given current density. Said otherwise, the 187
best catalyst should be the one which operates at the highest efficiency (η), η being 188
defined as the ratio of the operating voltage (E) to the theoretical thermodynamic 189
voltage (E_{eq}): $\eta(\%) = (E/E_{eq}) \times 100$. In addition to the efficiency criterion, long- 190
term operation of a fuel cell is an equally important requirement. A desirable catalyst 191
should therefore be characterized with a high efficiency and also exhibit minimal 192
loss in activity over long-term use. 193

However, the costs for installation of a fuel cell prototype are fairly high, and the 194
devise is fairly expensive to operate. Additionally, long-term stability tests are 195
particularly time consuming, which would make preliminary evaluation of catalysts 196
using a fuel cell prototype unnecessarily costly, both resource-wise and time-wise. 197
Preliminary evaluation of catalysts for fuel cells therefore often involves indepen- 198
dent investigation of their half-cell reactions. A brief description of the methods 199
that are most commonly used to investigate catalysts for the oxygen half-cell 200
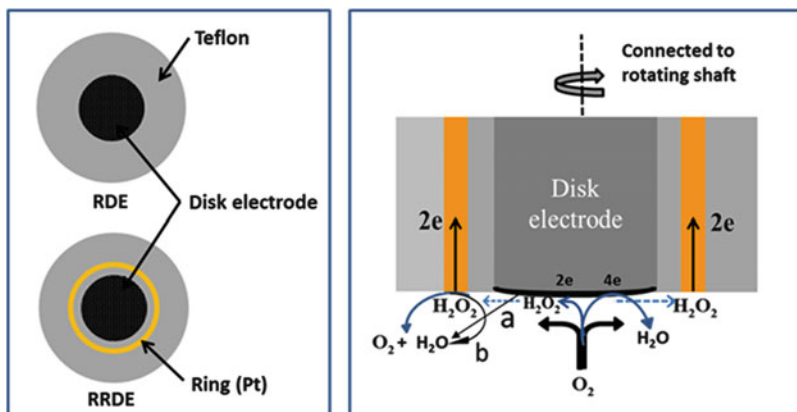reaction follows in the next section. 201

Fig. 7.5 Schematic representation of the RDE and RRDE (*left panel*) and of the possible reactions that take at the RRDE during ORR (*right panel*)

7.1.3 Determination of the Selectivity of O_2 Electroreduction

Ordinarily, the selectivity of ORR is determined by means of rotating disk electrode (RDE) or rotating ring-disk electrode (RRDE) voltammetry. The RDE is designed to boost the diffusion of an electroanalyte in conditions where an electrochemical reaction is limited by diffusion of the analyte to the electrode. In RRDE, a ring (often platinum) surrounds the disk electrode with an insulating material (usually Teflon) between them (Fig. 7.5).

During rotation of the electrode, the electrolyte is tangentially drawn to the disk electrode and radially swept away from it under controlled hydrodynamic conditions. Levich showed that the diffusion limited current (i_d) measured at a smooth disk electrode under controlled rotation is related to the angular velocity speed of rotation of the electrode according to Eq. (7.1) [27]:

$$i_d = 0.62nFAD_0^{2/3}\omega^{1/2}v^{-1/6}C_0 \tag{7.1}$$

where n is the number of electrons exchanged per molecule, F is the Faraday constant, A is the surface area of the electrode, D_0 is the diffusion coefficient of the electroanalyte, ω is the angular velocity of the electrode, v is the kinematic viscosity of the electrolyte, and C_0 is the bulk concentration of the electroanalyte. For a reaction which is essentially under diffusion limitation, a graph of i_d against $\omega^{1/2}$ yields a straight with a slope $= 0.62nFAD_0^{2/3}C_0v^{-1/6}$ from which n may be determined. Note that the coefficient 0.62 is used when ω is expressed in rad s^{-1}, while 0.21 is used when ω is expressed in revolution per minute (i.e., $0.62 \times (2\pi/60)^{1/2} = 0.21$) [28]. A more commonly used approach employs a modification form of Eq. (7.1), called the Levich-Koutecky analysis [Eq. (7.2)], for reactions which are under mixed kinetic

and diffusion control, where i is the measured current, i_k is the kinetic current defined 224
by Eq. (7.3), and i_d is the term in Eq. (7.1): 225

$$\frac{1}{i} = \frac{1}{i_k} + \frac{1}{i_d} \text{ or } \frac{1}{i} = \frac{1}{i_k} + \frac{1}{B\sqrt{\omega}} \tag{7.2}$$

$$i_k = knAFC_0 \tag{7.3}$$

From Eq. (7.2), a graph of the inverse of the measured current at a given 226
potential i^{-1} against $\omega^{-1/2}$ gives a straight line with a slope of B^{-1} from which n 227
can be determined and i_k^{-1} as the intercept on the i^{-1} axis [27]. 228

The RRDE is designed in such a way that under the hydrodynamic conditions, an 229
electroactive species generated at the disk may be detected at the ring electrode. The 230
species generated at the disk electrode must therefore be sufficiently long-lived to be 231
able to traverse the radius of the disk electrode and be detected at the ring. For the case 232
of the ORR, the ring electrode is always poised at a potential where any H_2O_2 233
generated at the disk is oxidized at the ring. The fraction of H_2O_2 generated during 234
ORR is calculated from Eq. (7.4), while the number of electrons transferred (n) is 235
obtained from Eq. (7.5): 236

$$XH_2O_2 = \frac{2I_R/N}{I_D + I_R/N} \tag{7.4}$$

$$n = \frac{4i_{O2}}{i_{H2O2}/N + i_{O2}} \tag{7.5}$$

where N is the collection efficiency of the ring electrode, I_R is the ring current, I_D is 237
the disk current, while i_{O2} is the electrocatalytic oxygen reduction current at the 238
disk, and i_{H2O2} is the corresponding ring current due to H_2O_2 oxidation at a specific 239
potential. The value of N is normally supplied by the manufacturer but it is 240
advisable to verify it as often as possible using a suitable redox pair [29]. 241

RDE and RRDE are very convenient voltammetric methods for studying the 242
mechanism and kinetics of ORR and are by far the most widely used methods. 243
However, it is important to bear in mind that the underlying mathematical 244
formulations of these methods are theorized for smooth electrode surfaces under 245
laminar flow hydrodynamics. There are many examples in recent literature where 246
RDE and RRDE have been used to study catalyst films for which turbulent flow 247
hydrodynamics is quite obvious. The collection efficiency of RRDE for microscopi- 248
cally disordered films, for example, very porous materials and irregularly built-up 249
films (as may be the case for catalysts modified with nanocarbons such as carbon 250
nanotubes and graphenes), is likely to be determined erroneously due to sporadic 251
hydrodynamics. Therefore, the quality of a given catalyst film has a great influence on 252
the correctness of results obtained from RDE and RRDE. It is generally 253
recommended that catalyst films for RDE and RRDE studies should be as thin as 254

255 possible [29]. Thick films may lead to increased mass-transport resistance through the
256 catalyst layer and incomplete utilization of the catalyst which certainly lead to
257 incorrect interpretation of results. These factors have to be considered critically
258 when performing and interpreting RDE and RRDE measurements. A depiction of
259 the possible processes that occur during the electroreduction of oxygen at RRDE
260 electrodes is schematically shown in Fig. 7.4 to draw attention to some possible
261 sources of error in treatment and interpretation of RRDE results. If O_2 is reduced by
262 the transfer of two electrons to form H_2O_2, at least four competing reactions may
263 follow and these include a competition between further electroreduction of H_2O_2 and
264 its disproportionation on the disk, and if the H_2O_2 makes it to the ring, a competition
265 between its electrochemical detection and disproportionation takes place since H_2O_2
266 is known to disproportionate on Pt surfaces. Therefore, the amount H_2O_2 detected at
267 the ring is likely to be much lower than the amount actually produced because of the
268 competing reactions. The magnitude of the error encountered in the determination of
269 n and H_2O_2 using RRDE is likely to be even larger the less smooth the catalyst film is.
270 However, in the absence of a more reliable method for studying the mechanism and
271 kinetics of ORR, RDE, and RRDE voltammetries continue to be useful and handy. In
272 the face of these drawbacks, several groups have proposed the use of scanning
273 electrochemical microscopy (SECM) to study the selectivity of electrocatalysis of
274 ORR [30–34].

7.2 From Model Structures to Active N$_4$-Metallomacrocyclic Catalysts

277 There is a vast amount of scientific literature about ORR catalysis by metalloma-
278 crocyclic. As mentioned earlier in the introduction, a variety of factors influence
279 the ORR activity of these complexes, including the method used for immobiliza-
280 tion of the complex, the pH of the electrolyte, and the conditions and quality of the
281 experiments among others. As such, there is some ambiguity concerning the ORR
282 selectivity of some complexes. In the next Sects. 2.1–2.4, a discussion of ORR
283 catalysis by N$_4$-metallomacroyclic complexes is given with special emphasis
284 placed upon those complexes and their design aspects which facilitate the four-
285 electron reduction of oxygen. Nature achieves facile reduction of O_2 to water at
286 very high turnover frequencies in the terminal respiration chain by cytochrome
287 c oxidases (CcO) at their heme (Fe a$_3$)/Cu (Cu$_B$) bimetallic active site (Fig. 7.6a).
288 This makes CcO interesting model systems to emulate, in what should be appro-
289 priately termed as bioinspired catalyst design. The next section gives a brief
290 insight of the electrocatalysis of oxygen reduction by CcO and the progress
291 attained in the biomimetic design of artificial heme/Cu-like catalysts for oxygen
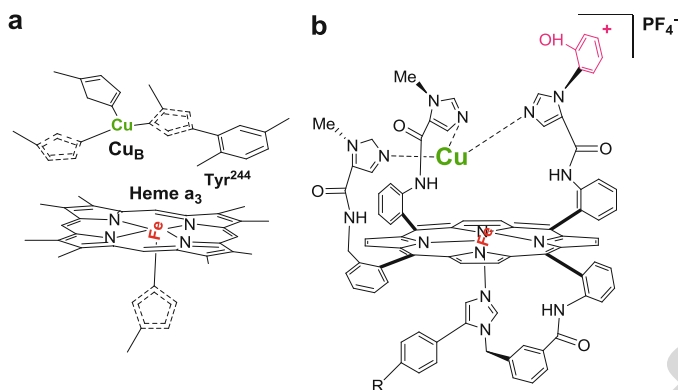292 reduction.

Fig. 7.6 Active structure of cytochrome c oxidase (**a**) and of a synthetic analog of cytochrome c oxidase (**b**) [35]

7.2.1 *Oxygen Reduction by Cytochrome c Oxidases*   293

Natural cytochrome c oxidases (CcO) catalyze the reduction of oxygen at their 294
heme a_3/Cu$_B$ (Fig. 7.6a) bimetallic site directly to water without the release of 295
superoxide or peroxide. The Fe–Cu distance in CcO varies in the range of 296
~4.9–5.3 Å [36], depending on the redox states of the metal ions and ligation 297
thereof, depending on the protein environment. 298

Recent work by Collman and Ghosh [35] has provided additional evidence that 299
the active site in CcO is comprised of a heme a_3 of an iron porphyrin and Cu (Cu$_B$) 300
coordinating three histidine groups with one of the histidine groups bound to a 301
posttranslationally modified tyrosine residue (Fig. 7.6b). It is reported that the 302
primary role of the redox centers is to rapidly provide the four electrons needed to 303
reduce oxygen directly to water without the release of toxic superoxide or peroxide 304
species. 305

The first step of the reduction process involves adsorption of oxygen at the 306
reduced Fe^{II}/Cu^I center to form an Fe^{III}–O$_2^-$ superoxide adduct with subsequent 307
formation of an intermediate comprised of oxidized Cu^{II}, an Fe^{IV}=O ferryl radical, 308
and a peripheral phenoxide radical (Fig. 7.7). The oxidized intermediate is then 309
reduced directly to water by simultaneous transfer of four electrons [35]. 310

Tremendous effort has been devoted to synthesize artificial catalysts which can 311
achieve reduction of oxygen directly to water by mimicking the active site of CcO 312
[35]. A key motivation of this endeavor has also been to use the CcO synthetic 313
analogs as biomimetic models to probe the structure and function of CcO in the 314
respiration chain. After an enduring effort spanning about three decades, successful 315
synthesis of a functional heme/Cu analog with the ability to reduce oxygen directly 316
to water at physiological conditions without generation of toxic peroxide and 317
superoxide species was reported [35–39]. It is generally believed that natural 318
enzymes exhibit unique flexibility, with the ability to sustain long range open-to- 319
closed conformational changes, which is necessary for binding and catalyzing the 320
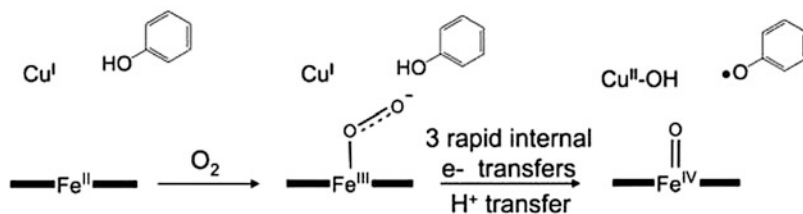
Fig. 7.7 A simplified mechanism leading to formation of the oxidized intermediate in the course of oxygen reduction at the active site of a functional heme/Cu analog of CcO [35]

321 reaction of small molecules [40]. Synthetic mimics of the heme/Cu active site in
322 CcO must therefore be faultlessly designed with such conformational flexibility as
323 to facilitate adsorption of oxygen, retention of partially reduced oxide species
324 (PROS) intermediates until final products are formed, and release of the products.
325 Artificial analogs of the heme/Cu sites in CcO have tended to be rather rigid, devoid
326 of this conformational flexibility. A number of factors which complicate replication
327 of the heme/Cu site of the CcO system in biomimetic design of functional heme/Cu
328 analogs for oxygen reduction have been discussed [39]. Functional analogs of CcO
329 incorporating dissimilar metal centers other than a heme/Cu active site have also
330 been reported [41]. The success achieved in synthesizing functional CcO analogs
331 and in the elucidation of their mechanism for oxygen reduction not only is useful for
332 understanding the role of CcO in the terminal respiration chain but also gives new
333 impetus to the design of effective molecular catalysts for four-electron reduction of
334 oxygen.

335 *7.2.2 Oxygen Reduction by Bimetallic Cofacial Porphyrins*

336 Cofacial metalloporphyrins refers to a molecular arrangement whereby the metal ions
337 of two independent planar metalloporphyrins exist face-to-face with each other. This
338 molecular configuration may arise by spontaneous molecular arrangement, for exam-
339 ple, due to π–π stacking, or by employing special synthetic schemes [42]. Dicobalt
340 cofacial diporphyrins hinged on amide bridges were the earliest bimetallic
341 diporphyrins with close semblance to the heme/Cu system that achieved four-electron
342 reduction of oxygen to water in acidic electrolytes at remarkably low overpotentials
343 [43]. Minor alterations in the dicobalt diporphyrin structures are reported to drasti-
344 cally poison the potency of the catalysts or cause them to revert to two-electron
345 oxygen reduction catalysts [44]. Selection of the right anchoring system for the two
346 individual cobalt porphyrin units to achieve just the right interplanar conformational
347 separation between them is one critical factor in designing dicobalt cofacial
348 diporphyrins with the ability to reduce oxygen to water. The first successful bridging
349 system for two dicobalt diporphyrins was reported by Collman et al. [42, 43] and
350 comprised of two diametrically positioned four-atom amide chains. The potential at

Table 7.2 Dicobalt cofacial porphyrins with a high selectivity for direct four-electron reduction of oxygen

Electrocatalyst	Medium	$E_{1/2}$ (V) vs. NHE	n	References
Co_2FTF4	0.5 TFA	0.71	3.9	[43]
Co_2DPB	0.5 TFA	0.70	3.7	[45]
Co_2DPA	–	0.67	3.7	[45]
Co_2DPD	0.5 M $HClO_4$	ca. 0.57	4	[40]
Co_2DPX	0.5 M $HClO_4$	ca. 0.58	4	[40]
$[Ir(OEP)]_2DDAB$	0.5 M H_2SO_4	0.80	4	[46]
$[Ir(OEP)]_2$	0.1 TFA	0.57	4	[47]

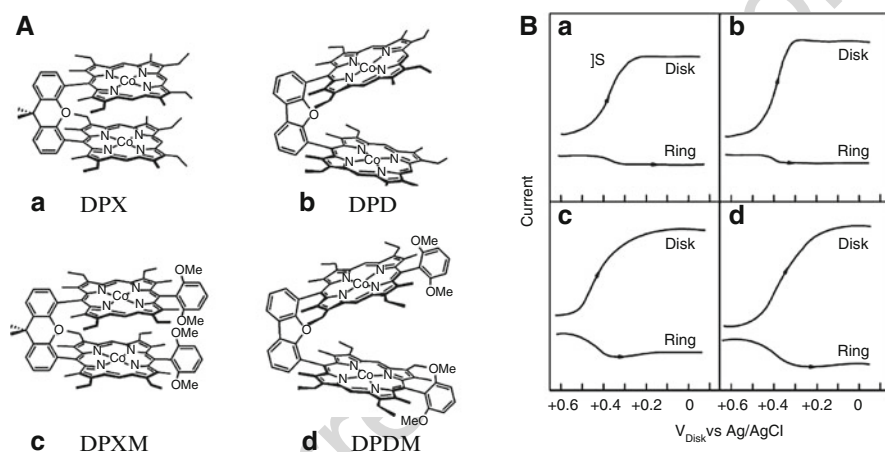*DDAB* didodecyldimethylammonium bromide, *TFA* trifluoroacetic acid

Fig. 7.8 (**A**) Examples of dicobalt cofacial bisporphyrins: *DPX* diporphyrin xanthene (a); *DPD* diporphyrin dibenzofuran (b); *DPXM* diporphyrin xanthene methoxyaryl (c); *DPDM* diporphyrin dibenzofuran methoxyaryl (d). (**B**) Rotating ring-disk voltammograms of O_2 reduction at pyrolytic graphite disks modified with (a), (b), (c), and (d) [48]

which oxygen reduction commences in these complexes is substantially more posi- 351
tive than the standard potential of the O_2/H_2O_2 couple ($E = 0.68$ V vs. SHE) which 352
thermodynamically precludes production of hydrogen peroxide by any mechanism. 353
Table 7.2 shows examples of dimetal cofacial porphyrins which achieve the four- 354
electron reduction of O_2 to water at substantially low overpotentials. 355

If one or both cobalt atoms were replaced by other metal atoms, hydrogen peroxide 356
was formed either as the main product or as an intermediate. Chang et al. [40] found 357
that dicobalt diporphyrins anchored on dibenzofuran (DBD) and xanthene (DPX), 358
Fig. 7.8A, exhibited remarkable conformational flexibility, and in both cases, the 359
complexes were able to reduce oxygen directly to water despite having large 360
differences (~4 Å) in the interplanar separation of their metal centers. Two other 361
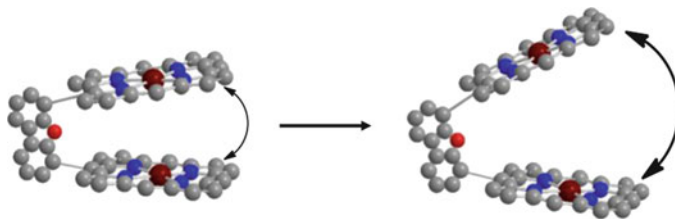anchoring systems, anthracene and bisphenylene, have also been successfully used to 362

Fig. 7.9 Illustration of the flexibility of dicobalt cofacial porphyrins with a dibenzofuran bridging system showing the "Pac-Man effect." *White* = hydrogen, *gray* = carbon, *red* = oxygen, *blue* = nitrogen, and *crimson* = Co

design four-electron oxygen reduction "pillared" cobalt (II) cofacial diporphyrins, Fig. 7.8A [45, 49]. The flexibility of the dicobalt cofacial porphyrins anchored on DPD and DPX was attributed to the ability of these hinge-like frameworks (or pillared platforms) to considerably open their bite "the Pac-Man effect" as illustrated in Fig. 7.9 in accommodating exogenous ligands.

The effect of the type of anchoring system and porphyrin structure on the ORR activity of dicobalt cofacial diporphyrins can be observed in Fig. 7.8A. The ORR activity is drastically affected by the introduction of 2,6 dimethoxyphenyl groups to the *meso*-position of the porphyrin ring as can be seen by the increased anodic current registered at the ring. It is however not definitively clear whether it is the electronic changes or steric effects which lead to this sharp drop in activity. Some quantitative results showing the effect of the type of anchoring system on the ORR activity of dicobalt cofacial porphyrins have been reported in the review by Collman et al. [50].

The two cobalt centers in dicobalt cofacial diporphyrins have been reported to act in concert in order to achieve four-electron reduction of oxygen [51, 52]. One of the sites reportedly functions as a Lewis acid to stabilize the intermediate(s) in the cavity, ensuring that it does not dissociate before completion of the reaction [53]. To corroborate the dual-site postulate and specificity of the reaction site, a parallel type of mechanism involving both the two- and four-electron reduction was observed when one of the Co(III) centers in Co_2FTF4 was replaced by Al(III) [53]. A simplified scheme of the proposed mechanism of oxygen by dicobalt cofacial porphyrins is shown in Fig. 7.10 [48].

Electrocatalysis of O_2 reduction using bimetallic cofacial diporphyrins bearing dissimilar metal ions has been investigated by some groups. Using anthracene as the bridging system, Ni et al. [54] investigated the influence of the nature of the metal centers including Co–Co, Co–Cu, Co–Fe, Fe–Fe, and Fe–H_2 on the electrocatalysis of ORR by cofacial dimeric porphyrins. The cofacial dimeric porphyrin was found to reduce oxygen to hydrogen product as the final product. The other complexes, namely, Co–Fe, Fe–Fe, and Fe–H_2, were reported to catalyze the reduction of O_2 by a parallel mechanism involving both the two-electron and the four-electron reduction pathways. The researchers reported that for those catalysts which reduced O_2 to water, H_2O_2 was not formed as an intermediate.
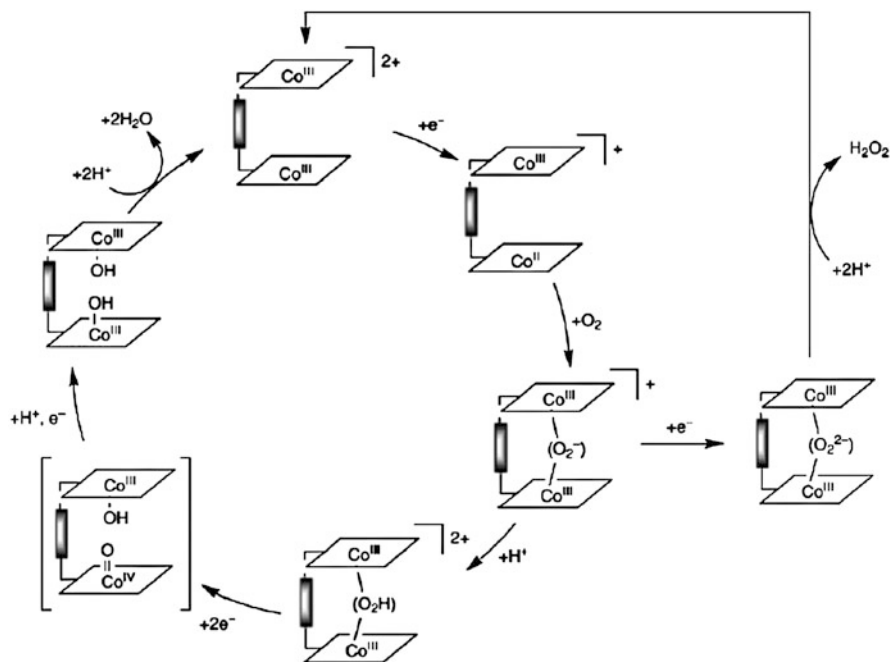
Fig. 7.10 Proposed mechanism for oxygen reduction at an active site of a dicobalt cofacial diporphyrin (adopted from [48])

A major drawback associated with dicobalt cofacial diporphyrins is their drastic 396
decline in activity when adsorbed on other electrode surfaces other than edge-plane 397
graphite (EPG). The catalysts have been reported to revert to two-electron reduction 398
catalysts when adsorbed on other electrode surfaces other than EPG [50]. This has 399
led to the conclusion that axial ligation of surface oxygen groups on EPG to the 400
cobalt ion bears a significant contribution to the ORR activity of these complexes 401
[50]. A second disadvantage is that these complexes are active in limited potential 402
and pH windows outside of which they become readily deactivated. In a particular 403
study which investigated the influence of site availability of these complexes for 404
oxygen adsorption and for axial ligation on their activity for oxygen reduction, that 405
is, whether the sites were located inside or on the outside of the cavity, it was found 406
that four-electron reduction of oxygen was only possible when the sites inside the 407
cavity were both available for interaction with oxygen. As with monomeric mono- 408
nuclear porphyrins, dicobalt cofacial diporphyrins also gradually lose their activity 409
upon repetitive potential cycling for a few cycles. Pretreatment of the active 410
catalysts with hydrogen peroxide was found to rapidly deactivate them indicating 411
that the mechanism of their deactivation involves chemical attack by peroxide and 412
superoxide species. Despite all these existing drawbacks, the success achieved thus 413
far should stimulate enthusiasm for synthesis of molecular heme/Cu or heme/Cu- 414
like analogs of CcO and dinuclear cofacial porphyrin which can function under the 415

416   conditions desirable for technological applications. As proposed way back in the
417   original work by Collman et al. [43] it should be possible to modulate the ORR
418   activity of the dicobalt cofacial porphyrins by judicious modification of the por-
419   phyrin ring and possibly by exploration of other bridging groups.

7.2.3   ORR by Simple N$_4$-Metallomacrocyclic Complexes

421   There is a large amount of literature available about the pathways for oxygen
422   reduction by N$_4$-metallomacrocyclic complexes, with the reported results conflicting
423   in some cases, which complicates a balanced review of the work. Additionally, the
424   activity and stability of N$_4$-metallomacrocyclic complexes are affected by a variety of
425   factors as spelt out in the introduction. This makes it difficult to make reliable cross-
426   laboratory comparisons. However, by and large, the number of simple N$_4$-metalloma-
427   crocyclic complexes that can achieve the reduction of oxygen exclusively to water
428   without generation of substantial amounts of hydrogen peroxide is generally very
429   limited. Much of the attention in this section is devoted to research frontiers in view
430   of promising simple N$_4$-macrocyclic catalysts that can achieve four-electron reduc-
431   tion of oxygen as this is the primary desire of many researchers in the field. To
432   simplify our task, bearing in mind that thorough coverage of all the important works
433   reported over the last four decades by various authors cannot be achieved faultlessly,
434   emphasis of the discussion was placed more on specific structural properties or
435   special catalyst preparation procedures that achieve four-electron reduction of oxy-
436   gen either (a) in a direct four-electron reduction process, or (b) in a series process via
437   hydrogen peroxide as an intermediate with its further electrochemical reduction to
438   water or dismutation to water and oxygen, or (c) in a parallel type mechanism
439   involving both (a) and (b). Unique cases involving sophisticated modifications, or
440   otherwise, by means of which oxygen is reduced by the transfer of four electrons have
441   also been included in as far as we could access the concerned literature. The rationale
442   for discussing the electrocatalysis of oxygen reduction by these complexes in slight
443   detail was to draw attention to their important properties which furnish them with the
444   unique ability to facilitate the four-electron reduction of oxygen.

7.2.4   Direct Four-Electron Reduction of O$_2$ by Simple
Monomeric N$_4$-Macrocycles

447   It has been shown in several studies that the ORR activity of metallomacrocyclic
448   complexes is very dependent on the pH of the electrolyte. Therefore, a given
449   metallomacrocyclic complex may catalyze the reduction of oxygen via the four-
450   electron reduction in a specific pH window, outside of which, it may only afford to
451   it via the two-electron pathway. This is particularly true for Fe and Co porphyrins
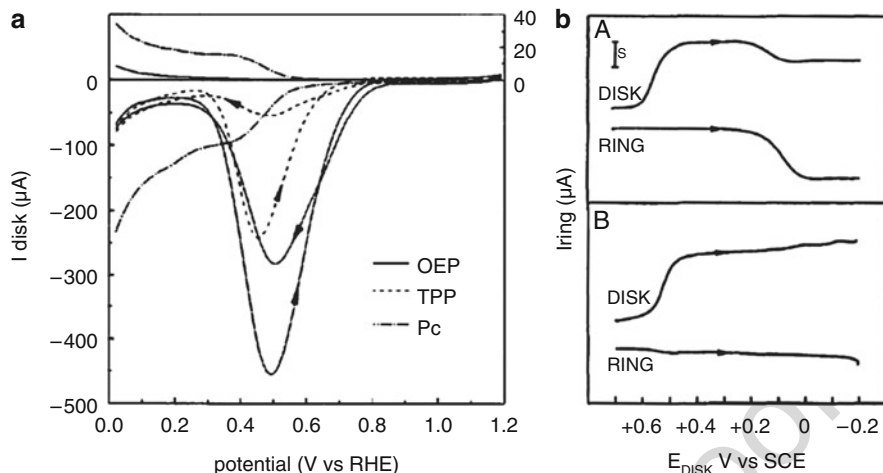
Fig. 7.11 (**a**) Rotating ring-disk voltammograms of iridium chelates irreversibly adsorbed on pyrolytic graphite (Cp) in 0.5 M H_2SO_4 at a rotation of 16 rps and scan rate of 10 mV s^{-1} [56] (reproduced with permission of Elsevier); (**b**) rotating ring-disk voltammograms of a Pt (*ring*) and graphite (*disk*) coated with DDAB and [Ir(OEP)]$_2$ (1.3×10^{-9} mol cm^{-2}) *upper panel* (A) and *lower panel* (B) Pt ring (*uncoated*)-Pt disk in 0.5 M H_2SO_4 saturated with air. The Pt rings were maintained at 1.0 V in both cases [46]

and phthalocyanines. Fe phthalocyanines generally reduce oxygen via the four- 452
electron pathway under alkaline conditions, whereas the two-electron transfer 453
pathway is predominant under acidic conditions. This is quite the oppositee for 454
Co phthalocyanines which show a higher selectivity towards the four electron 455
trasfer pathway in acidic electrolytes wheras they are essentially two-electron 456
reduction catalysts under alkaline conditions. This subject will be discussed in 457
details in Chap. 3. Most simple monomeric, monometallic N_4-metallomacrocyclic 458
complexes can only achieve the reduction of oxygen to hydrogen peroxide by the 459
transfer of two electrons. A few metallo N_4-macrocyclic complexes can however 460
catalyze the reduction of oxygen in a direct four-electron transfer process and they 461
constitute the subject of discussion in this section. 462

Many iridium porphyrins, specifically Ir(OEP)R, R = H, alkyl or aryl derivatives, 463
and Ir(OEP)I and Ir(OEP)OOH, catalyze the direct four-electron reduction of oxygen 464
at substantially low overpotentials [55]. With the exception of Ir(OEP)H, the rest of 465
the complexes require preconditioning at specific potentials to be activated, the 466
required conditioning potential varying depending on the nature of substituent groups. 467

According to studies by Collman et al. [47] Ir(OEP)R complexes specifically 468
required conditioning at high positive potentials (>0.8 V vs. NHE), while Ir(OEP)I 469
and Ir(OEP)OOH required conditioning at negative potentials (<−0.2 V vs. NHE) 470
to be activated. As can be seen in Fig. 7.11a, Ir(OEP)H has been reported to exhibit 471
the best activity similar to or better than that observed for dicobalt cofacial 472

t3.1 **Table 7.3** Metallomacrocyclic complexes with high activity and significantly low overpotentials for oxygen in acidic electrolytes

Electrocatalyst	Medium	$E_{1/2}$ (V) vs. NHE	(n)	References
Ir(OEP)H	0.1 M TFA	0.72/0.8	3.9	[55]
IrTPP	0.1 M TFA	0.48	NR	[47, 56]
Ir(OEP)R, R=OOH, Ph	0.1 M TFA	0.54	NR	[47]
CoP	1 M HClO$_4$	0.75	3.8	[57]
CoTMeP	1 M HClO$_4$	0.64	3.3	[57]
[CoP(PyRu(NH$_3$)$_5$)$_4$]	0.5 M HClO$_4$	0.47	NR	[52]
[CoP(PhCNRu(NH$_3$)$_5$)$_4$]	0.5 M HClO$_4$	0.58	NR	[52]
[CoP(py-CH$_3$)$_4$(Os(NH$_3$)$_5$)$_{\sim 2}$]	0.5 M HClO$_4$	0.59	NR	[52]

t3.11 *NR* not reported, *n* number of electrons transferred

porphyrins [47, 55]. It was reported in a study by Shi et al. [46] that the presence of a cationic surfactant (DDAB) improved both the activity and stability of Ir(OEP)H and also widened its active potential window, Fig. 7.11b.

The dimeric form of Ir(OEP), [Ir(OEP)]$_2$, also catalyzes the direct four-electron reduction of oxygen, but unlike its monomer, it does not require any conditioning. As shown in Fig. 7.11a, the iridium chelate complexes become severely but reversibly deactivated at low potentials [56]. Their activity is not however affected by pH as dramatically as the dicobalt cofacial diporphyrin complexes. As with the case for Co$_2$FTF catalysts, it has been reported that when the Ir(OEP)R catalysts are adsorbed on other electrode surfaces other than EPG, their activity declines to two-electron reduction catalysts. Quite surprisingly, the main product of oxygen reduction was reported to be hydrogen peroxide after pyrolysis of Vulcan supported IrOEP and IrTPP. This is a rather peculiar case since the activity of most N$_4$-metalloporphyrins increases upon their pyrolysis. It has also been reported that the Ir complexes are unstable in air, losing all their activity after a few months. The four-electron reduction of oxygen by iridium porphyrins has been attributed to a single site which facilitates the adsorption of oxygen on Ir(II)in a side-on configuration, with scission of the O–O bond being a likely step in the mechanism.

Unfortunately, Ir is one of the rarest and most expensive metals which would render its use very costly. Nonetheless, the complex should serve as a suitable model, such that theoretical and experimental knowledge gained from its study may serve to tailor the synthesis of improved catalysts. Table 7.3 lists some metallomacrocyclic complexes which accomplish the reduction of oxygen via the four-electron transfer pathway in acidic electrolytes.

The other monomeric mononuclear porphyrins which mediate the four-electron reduction of oxygen are cobalt porphyrin (CoP) and cobalt *meso*-tetramethyl porphyrin (CoTMeP), with CoP exhibiting a higher activity than CoTMeP [57]. The unexpectedly high activity of CoP has been attributed to its likely spontaneous dimerization to produce a more catalytically active species. The synthesis of CoP or its free base (porphine) is quite challenging specifically regarding the attainable yield and purity, which makes it overly expensive for a nonprecious metal catalyst. Another drawback is that the catalyst is highly susceptible to oxidative degradation

which severely affects its merit. In a later study which compared the ORR activity of several *meso*-tetraalkyl cobalt porphyrins by the same group, activity was found to follow the order CoP > CoTmeP > CoTBuP > CoTPrP > CoTEtP > CoPeP [16]. This led to the conclusion that the rate of adsorption of oxygen decreased as the bulkiness of the alkyl substituents increased. At the moment, there is no foreseeable strategy for improving the stability of CoP. Nevertheless, understanding its properties which furnish it with this exceptional activity deserves to be investigated in detail.

7.2.5 *Specially Modified N$_4$-Metallomacrocyclic Complexes*

Some studies have shown that certain modification procedures can be used to transform two-electron reduction metalloN$_4$-macrocyclic complexes into hybrid materials with the capability to reduce oxygen to water, either via the direct four-electron transfer pathway or in the series two-electron transfer pathway. Carbon nanomaterials, carbon nanotubes in particular [58–65], have been reported to significantly increase the catalytic oxygen reduction current, with a substantial reduction of the overpotential for ORR reported in some cases, as shown by the examples in Table 7.4.

Ozoemena's group has recently reported that MOCPcPt (where M = Fe, Ru) (Fig. 7.12a) supported on multiwalled carbon nanotubes afford the reduction of O$_2$ in a direct four-electron transfer process in 0.1 M NaOH [60, 61, 67]. There was no significant difference between the ORR activity at the FeOCPcPt and RuOCPcPt except that the latter gave a slightly higher kinetic rate constant ($\sim$3.6 $\times$ 10^{-2} cm s^{-1}) than the former ($\sim$2.8 $\times$ 10^{-2} cm s^{-1}).

The other material design strategies that have been reported to yield four-electron reduction metalloN$_4$-macrocyclic complexes include the use of supramolecular assembly [68, 69], by exploiting the electrostatic interaction between oppositely charged ions as in the work of D'Souza et al. [70] and Liu et al. [71]. D'Souza et al. reported that a 98 % selectivity of O$_2$ reduction to water was achieved when a dimeric porphyrin formed by electrostatic coupling of [*meso*-tetrakis(*N*-methylpyridyl) porphyrinato]cobalt tetrachloride ([Co(TMPyP]$^{4+}$ Cl$_4^-$) with tetrasodium *meso*-tetrakis(4-sulfonatophenyl)porphyrinato]cobalt ([(Na$^+$)$_4$[Co(TPPS)]$^{4-}$) was used as a catalyst for ORR (Fig. 7.12b) [70]. In a related study, Liu et al. reported the formation of a supramolecular complex [CoTBPyP][SiW$_{12}$O$_{40}$] by the electrostatic interaction of *meso*-tetrakis(4-*N*-benzylpyridyl)porphyrinatocobalt (CoTBPyP) and a polyoxometalate anion, silicotungstate (SiW$_{12}$O$_{40}$)$^{4-}$, which was capable of reducing O$_2$ to water. The application of supramolecular porphyrins for oxygen reduction has been reviewed by Araki and Toma [72].

The multinulear complexes reported by Shi and Anson are another interesting example of specially designed metalloN$_4$-macrocyclic complexes with exceptional activity for ORR. Cobalt (tetrakis(4-pyridyl)porphyrin), with four [Ru(NH$_3$)$_5$]$^{2+}$ and ([(NH$_3$)$_5$Os]$^{n+}$ (*n*) 2, 3) groups around the porphyrin periphery, generally termed as

AU2
AU3
AU4

Table 7.4 Comparative onset potentials and current densities for MPc and MPc-CNT hybrid catalysts

MPc/CNT catalyst	Onset potential/V (vs. Ag|AgCl sat. KCl)	E_p/V (vs. Ag|AgCl sat. KCl)	Current density (mA cm^{-2})	References
NanoFePc	−0.2	−0.18	−0.6	[66]
NanoFePc-MWCNT	−0.05	−0.15	−1.7	
FeOBSPc	−0.2	−0.22	−0.5	[65]
FeOBSPc-MWCNT	0.0	−0.15	−1.4	
PtFeOCPc	−0.1	−0.30	−0.6	[61]
PtFeOCPc-MWCNT	0.0	−0.10	−1.2	

The current densities were measured at the stated peak potential (E_p/V Ag/AgCl, sat. KCl)
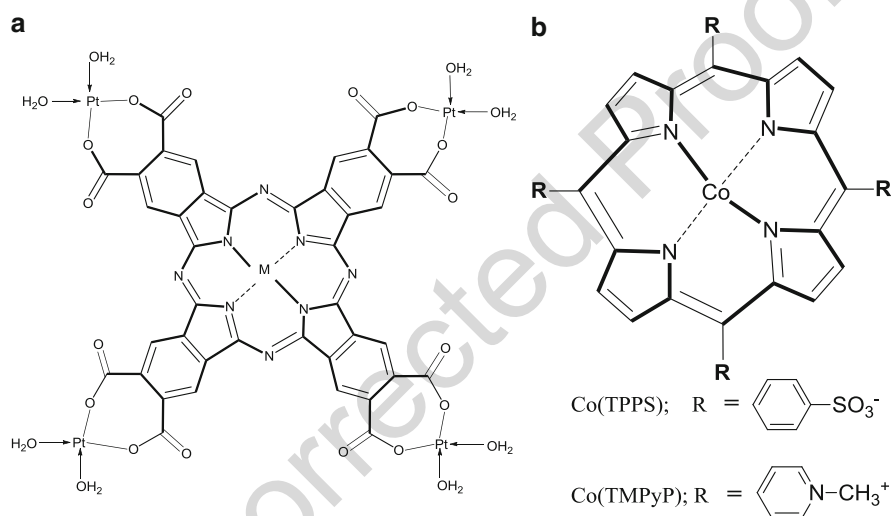
Fig. 7.12 (**a**) Structure of metallo-tetrakis-(diaquaplatinum)octacarboxy phthalocyanine (MOCPcPt, where M = Fe, Ru) and (**b**) structure of Co(TPPS) and Co(TMPyP)

"multinuclear catalysts" reduce oxygen nearly exclusively to water [52, 73–76]. As shown in Fig. 7.13b, the evident increase in the diffusion-limited current for oxygen reduction at the disk and the large decrease in the anodic current at the platinum ring clearly confirm that modification of CoP(py)$_4$ with [Ru(NH$_3$)$_5$]$^{2+}$ converts it from a predominantly two-electron O$_2$ reduction catalyst to a nearly exclusively four-electron reduction catalyst with minimal generation of hydrogen peroxide.

The proposed mechanism for oxygen reduction by the multinuclear ORR catalysts is outlined in Fig. 7.14 for tetraruthenated [CoP(pyRu(NH$_3$)$_5$)$_4$]$^{8+}$ but is also applicable to osmiumated porphyrins.

The mechanism has been proposed to involve π-backdonation from Ru(II) or Os (II) to the oxygen adsorbed porphyrin adduct Co(II)–O$_2$, where the cobalt porphyrin is the site for oxygen reduction while Ru and Os serve as cocatalysts which affect
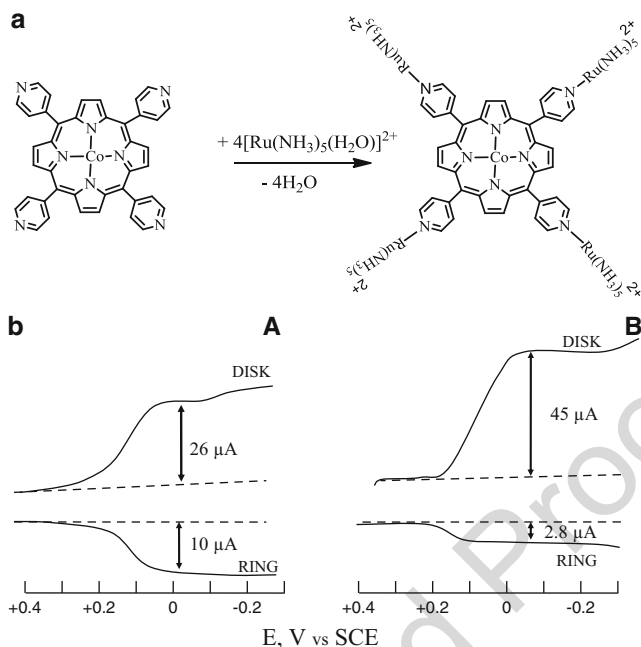
Fig. 7.13 (**a**) Reaction for conversion of $CoP(py)_4$ to $[Co^{II}P(pyRu^{II}(NH_3)5)^4]^{8+}$ (adopted from [52]). (**b**) RRDE voltammograms of (A) $CoP(py)_4$, (B) $[Co^{II}P(pyRu^{II}(NH_3)_5)_4]^{8+}$ (reproduced from [74])

$$\left[Co^{III}P(pyRu^{III}(NH_3)_5)_4 \right]^{13+} + e^- \rightleftharpoons \left[Co^{II}P(pyRu^{III}(NH_3)_5)_4 \right]^{12+} \qquad (1)$$

$$\left[Co^{II}P(pyRu^{III}(NH_3)_5)_4 \right]^{12+} + O_2 \rightleftharpoons \left[O_2CoP(pyRu^{III}(NH_3)_5)_4 \right]^{12+} \qquad (2)$$

$$\left[O_2CoP(pyRu^{III}(NH_3)_5)_4 \right]^{12+} + 4e^- \rightleftharpoons \left[O_2CoP(pyRu^{II}(NH_3)_5)_4 \right]^{8+} \qquad (3)$$

$$\left[O_2CoP(pyRu^{II}(NH_3)_5)_4 \right]^{8+} + 4e^- + 4H^+ \longrightarrow \left[Co^{II}P(pyRu^{II}(NH_3)_5)_4 \right]^{8+} + 2H_2O \qquad (4)$$

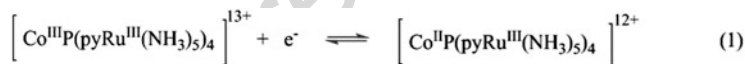$$\left[Co^{II}P(pyRu^{II}(NH_3)_5)_4 \right]^{8+} + O_2 \rightleftharpoons \left[O_2CoP(pyRu^{II}(NH_3)_5)_4 \right]^{8+} \qquad (5)$$
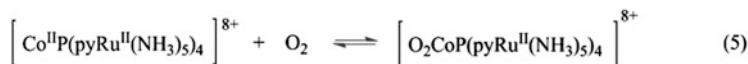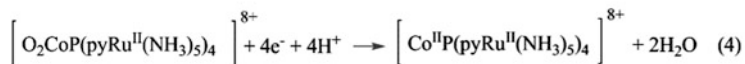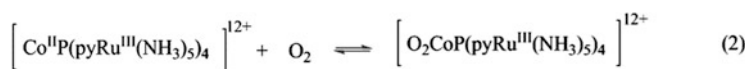
Fig. 7.14 Proposed mechanism for O_2 reduction by $[CoP(pyRu(NH_3)_5)_4]^{8+}$ and other related multinuclear complexes (reproduced from [52])
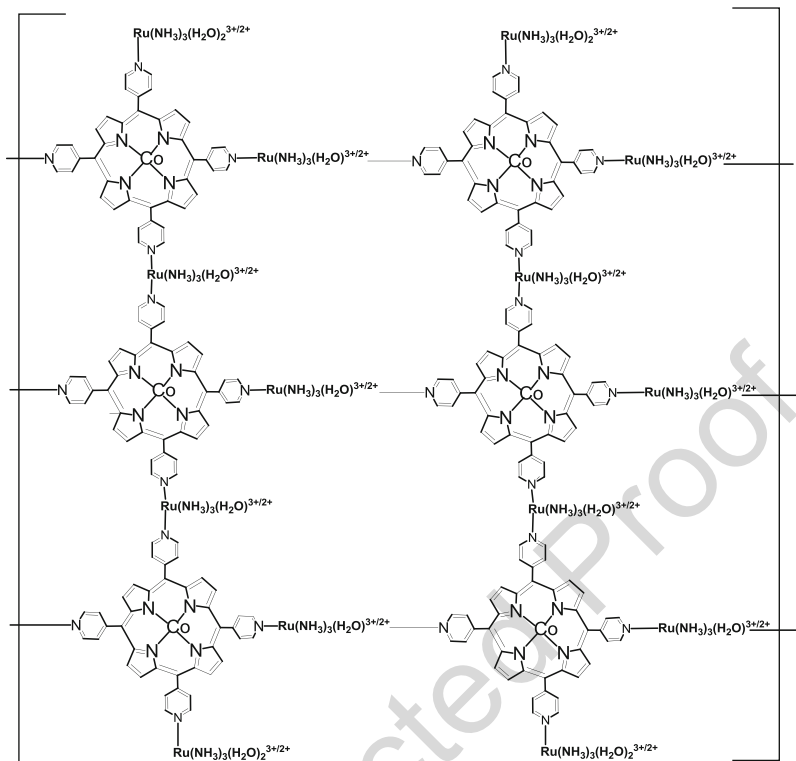
AU5

Fig. 7.15 Proposed structure of the supramolecular structure formed by complexation of *meso*-tetrakis((4-pyridyl)porphyrinato)cobalt (CoP(py)$_4$) with [Ru(NH$_3$)$_3$(H$_2$O)$_3$]$^{2+}$ on a graphite electrode   AU7

558 the relative rates of two competing pathways for oxygen. (1) The first step in the   AU6
559 mechanism involves generation of Co(II) porphyrin with subsequent adsorption of
560 oxygen on the active-site Co(II) in the next reaction (2). The next reaction
561 (3) generates the backbonding Ru(II) which drives the reduction of oxygen by
562 four electrons as shown in reaction (4) and finally, regeneration of the Co(II)–O$_2$ in
563 reaction (5). It has been proposed that the electronic effects produced by the
564 backdonation of the Ru(II) and Os(II) complexes on Co(II)–O$_2$ might be achieved
565 by other suitable electron-donating nonmetallic functional groups attached to the
566 porphyrin ring. It was however observed that differences in catalytic activity of
567 multinuclear complexes were correlated to the relative backbonding strengths of the
568 coordinated metal complexes but not on their relative reducing strengths.

569   Anson et al. postulated that their multinuclear catalysts described above may
570 actually be supramolecular porphyrins with a structure similar to that shown in
571 Fig. 7.15.

572   Most cobalt porphyrins can only reduce oxygen to hydrogen peroxide with no
573 further reduction or dismutation of the peroxide [77]. Some recent studies have
574 proposed a hybrid multifunctional catalyst incorporating a metallomacrocyclic

complex and Prussian blue (PB) or horseradish peroxidase (HRP) so that the hydro- 575
gen peroxide generated by the metallomacrocycle can be reduced further by the PB/ 576
HRP to water. For example, reduction of O_2 to H_2O was achieved by designing a 577
multicomponent-multifunctional catalyst incorporating carbon nanotubes (CNTs), 578
CoPIX, and PB. The CNTs provide a high surface area matrix for dispersion of the 579
catalysts [78]. 580

According to a study by Forshey et al. [79] electrodeposited iron *meso*-tetrakis 581
(*N*-methyl-4-pyridyl)porphyrin and electropolymerized *meso*-tetrakis(2-thienyl) 582
porphyrinato]cobalt(II) (pCoTTP) accomplsih the reduction of O_2 to water. The 583
ability of pCoTTP to reduce O_2 directly to water was attributed to a conducting 584
network of CoTTP nodal points where multiple layers are arranged in such a way 585
that they form suitable x.Co–Co bifacial binding clefts for O_2, thus allowing four- 586   AU8
electron reduction of oxygen to water. A study by Elbaz et al. [80] has reported 587
that Co(III) *meso*-tetra(*o*-aminophenyl)porphyrin (Co(III)TAPP) and Co(III) 588
(*p*-sulfonatedphenyl)porphyrin (Co(III)TPPS) incorporated into aerogel carbon 589
(AEG) electrodes by adsorption or electropolymerization achieved four electrons 590
of oxygen. 591

7.3 Fundamental Studies of O_2 Electroreduction by N$_4$-Metallomacrocyclic Complexes

592
593

The preceding section focused mostly on qualitative description of the dependence 594
of ORR activity on the structure of N$_4$-metallomacrocyclic complexes and some 595
special modification procedures which can be used to improve activity. In this 596
section, much of the discussion will focus on quantitative decription of the 597
parameters which influence the ORR activity of N$_4$-metallomacrocyclic complexes. 598
Specifically, the dependence of activity on the properties of the central metal ion 599
will be dicussed in relation to the driving force of the reaction. In addition to this, 600
the molecular orbital theory and the concept of intermolecular are used to describe 601
the interaction between oxygen the central metal ion in N$_4$-macrocyclic complexes 602
and how this interaction influences the ORR activity of the complex. 603

7.3.1 Effect of the Central Metal on the ORR Activity of N$_4$-Macrocylic Complexes

604
605

The electroreduction of oxygen by N$_4$-macrocylic complexes reaction is very sensi- 606
tive to the nature of the metal center in the complex. For Fe and Mn phthalocyanines, 607
at low overpotentials a four-electron reduction is observed with rupture of the O–O 608
bond [14, 81–83], without the formation of peroxide. In contrast Co, Ni, and Cu 609
phthalocyanines promote the reduction of O_2 only via two electrons to give peroxide 610

611 [14] as the main product of the reaction. Polymerized Co tetraaminophthalocyanines
612 promote the four-electron [84, 85] reduction, whereas polymerized Fe tetraami-
613 nophthalocyanines only promote the two-electron reduction [86] in contrast to their
614 monomeric counterparts. The net catalytic activity of metal macrocyclics is linked to
615 the redox potential of M(III)/(II) of the complexes, the more positive the redox
616 potential, the higher the activity. This trend is the opposite to what is expected from
617 a simple redox catalysis mechanism, which is generally observed for the reduction of
618 O_2 catalyzed by immobilized enzymes. The metal-N_4 chelates need to be supported
619 on a conducting support, like carbon or graphitic materials. Long-term stability is a
620 problem with N_4 chelates. Heat treatment in an inert atmosphere increases both the
621 stability and catalytic activity [87–92].

622   Even though a few studies have been carried out using the complexes in solution
623 [93], most studies have been performed with the metal chelates confined on an
624 electrode surface, generally graphite or carbon supports, since this is closer to the
625 situation in a fuel cell, where catalysts are absent in the electrolyte. Since the support
626 can act as an axial ligand, the properties of the complexes in solution or on the
627 adsorbed state could be different. So most studies discussed here have been carried
628 out with the complexes immobilized on graphite or carbon supports. Smooth
629 electrodes have been used to study mechanistic aspects of the reaction.

630 7.3.1.1 Interaction of O_2 with Active Sites and the Redox Mechanism

631 The one-electron reduction of O_2 to give superoxide is an outer-sphere reaction and
632 does not involve the interaction of the molecule with an active site on the electrode
633 surface. The electron transfer process probably occurs at the outer Helmholtz plane.
634 This process is observed in nonaqueous media or in strongly alkaline aqueous
635 solutions and is not relevant to fuel cell development since little free energy is
636 liberated in the process. In contrast, ORR occurring via the transfer of more than
637 one electron (two or four) is an inner-sphere reaction, involving the interaction of
638 the molecule and intermediates with active sites present on the electrode surface.
639 Since we are interested in discussing the electrocatalytic reduction of O_2, we will
640 focus our attention on the inner-sphere reduction processes.

641   O_2 interacts with the N_4 catalysts usually binding to the d orbitals of the central
642 metal in the macrocyclic structure. The energy of the interaction will depend on the
643 energy and the electronic density located on those orbitals. Figure 7.16 illustrates
644 some different possible interactions (end-on and side-on) of the orbitals of the oxygen
645 molecule with the orbitals of the metal in the M–N_4 molecule for end-on and side-on
646 interactions, respectively.

647   For end-on M–O_2 complexes (see Figs. 7.16 and 7.17), the most important
648 interaction for both σ and π bondings occurs with the π^* antibonding orbitals of
649 the O_2. The σ interaction is primarily between the metal $3dz^2$ and the in-plane
650 antibonding π_g^s orbital on the O_2, where the superscript "s" refers to whether or not
651 the orbital is symmetric (or antisymmetric) in relation to the MO_2 plane. This
652 interaction involves a transfer electron density from the metal to the O_2 molecule.

Fig. 7.16 End-on and side-on interactions of frontier orbitals of O_2 with the frontier orbitals of a metal site (reproduced from [94])
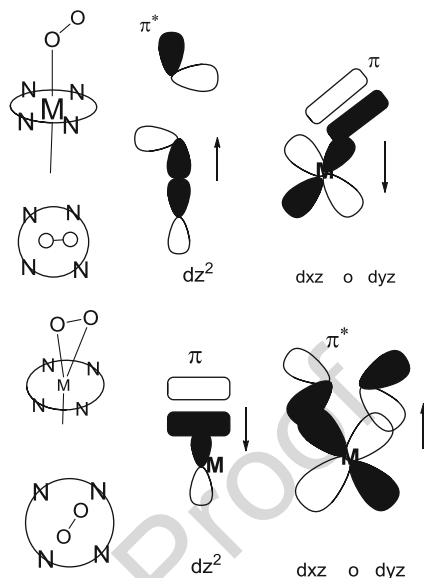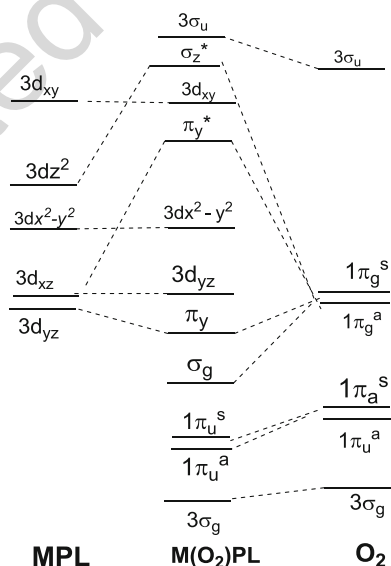
Fig. 7.17 Qualitative molecular orbital diagram for the end-on $M(O_2)PL$ dioxygen adduct. M = Fe, Co; P = porphyrin; L = NH_3 or imidazole (reprinted with permission from American Chemical Society [95])

The π interaction is primarily between the metal $3d_{yz}$ and the $1\pi_g^a$ (π antibonding 653
antisymmetric orbital) on the O_2 and can be viewed as a backbonding interaction. In 654
both of these interactions, the π_u^s and π_u^a (bonding π orbitals symmetric and 655
antisymmetric, respectively) play a lesser role in the composition of the bonding 656
orbitals [95]. In the case of the side-on interaction, a $3dz^2$ orbital of the metal 657
interacts with the $1\pi_s^u$ bonding orbital (backbonding interaction) and a 3 dxz with a 658

Fig. 7.18 Qualitative molecular orbital diagram for a side-on $Mn(O_2)PL$ dioxygen adduct (reprinted with permission from [95])
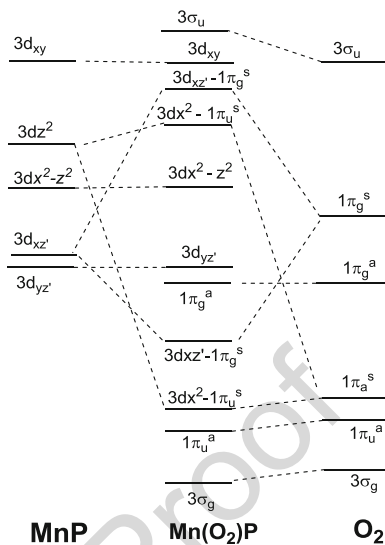
659   $1\pi_g{}^s$ antibonding orbital of oxygen as shown in Figs. 7.16 and 7.18. Figure 7.19
660   illustrates the optimized structural configurations for the O_2 adsorbed on FePc and
661   CoPc molecules according to calculations by Chen et al. [96].   AU9

662   The predominating interactions will weaken the O–O bond and increase the O–O
663   distance. The metal in the complex should be in the M(II) state, so, for example, in
664   alkaline solution a step will require the reduction of M(III):

$$M(III) - OH + e \rightleftarrows M(II) + OH^- \tag{7.6}$$
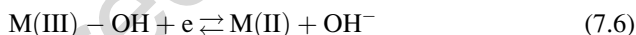
665   An adduct will be formed according to

$$M(II) + O_2 \rightleftarrows M(III) - O_2{}^- \text{ or } M(II) - O_2 \tag{7.7}$$

666   This adduct must be short-lived. Otherwise it will hinder further O_2 molecules
667   from interacting with the active site. The adduct will undergo reduction as follows:

$$M(III) - O_2{}^- + e^- \rightleftarrows M(II) + \text{intermediates} \tag{7.8}$$
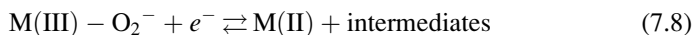
668   where M(II) is the active site. The last reaction shows the process in alkaline media
669   and could involve $M(II)–O_2$ instead of $M(III)–O_2{}^-$ especially when Co is the metal
670   center. In acid media the process will involve a proton. The scheme above is
671   applicable to Mn and Fe complexes. In the case of Co complexes, Co(III) is
672   probably not formed upon its interaction with the oxygen molecule since the Co
673   (III)/Co(II) formal potential is much more positive than the M(III)/(II) formal
674   potentials (M = Mn, Fe). However, step 2 is still important since the catalytically
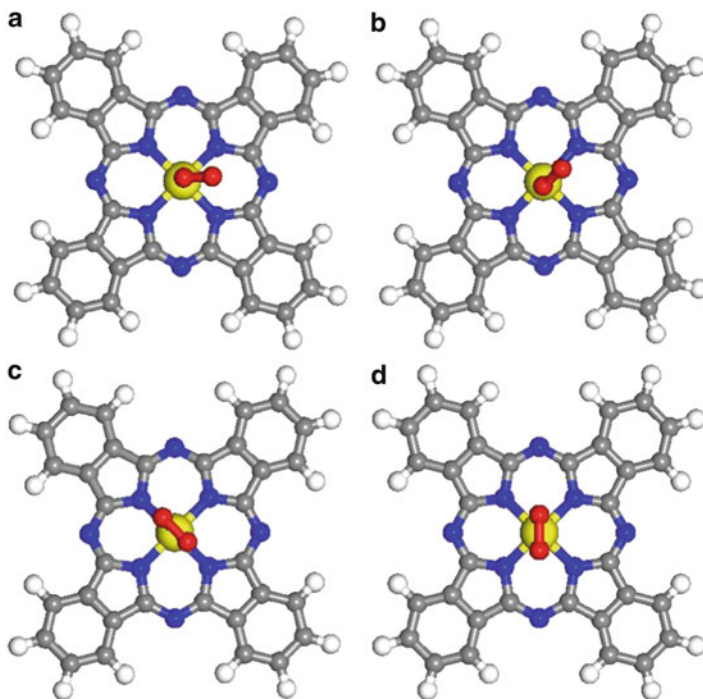675   active site is Co(II) [82, 97]. Density functional theory calculations [96] have

Fig. 7.19 Optimized structural configurations for the O_2 adsorbed on FePc and CoPc molecules. The *upper portion* shows two end-on configurations. The *lower portion* of the figure shows two side-on configurations. The *central yellow sphere* depicts the metal Fe or Co atom, the *central two red spheres* represent the adsorbed O_2 molecule, *blue spheres* represent N atoms, *gray spheres* represent C atoms, and *light white spheres* represent H atoms [96]

shown that that with CoPcs only end-on interaction is possible, whereas for FePc both end-on and side-on interactions are plausible. As it will be discussed further, only Mn and Fe phthalocyanines promote the four-electron reduction of O_2 and this can be attributed to a side-on interaction of O_2, particularly for Fe complexes.

Since the interaction of the oxygen with the active site involves a partial oxidation of the metal in the complex or at least a decrease of electron density in the metal upon interacting with O_2, it is interesting to compare the catalytic activity of metallomacrocyclic with their M(III)/(II) formal potential. Since the formal potentials are sensitive to the pH of the electrolyte, it should be measured in the same media in which the catalytic activity is examined [14, 20, 98]. Further, they should also be measured with the complex adsorbed on the electrode and not in solution phase. When comparing phthalocyanines, the Co and Fe derivatives show the highest activity for the reduction of O_2 but they behave differently. As pointed out above, Co complexes exhibit Co(III)/(II) transition that is far more positive than the onset potential for the reduction of O_2, whereas for Fe complexes the onset potential for the catalytic reduction of O_2 is very close to the Fe(III)/(II) transition [14, 82, 97, 99]. For both types of complexes, there is in situ spectroscopic evidence

for the reversible transition involving the M(III)/(II) couples [97, 100, 101]. For example, for Fe phthalocyanine adsorbed on ordinary pyrolytic graphite, Scherson et al. used Fe K-edge XANES (X-ray Absorption Near Edge Structure) recorded in situ in 0.5 M H_2SO_4 to prove the evidence for the redox transition of Fe(III)/(II) involving a metal-based orbital.

Many authors have discussed that a correlation should exist between the formal potential of the catalysts and its activity for ORR and it is yet not clear what sort of correlation should be expected. Reduction of O_2 should be observed at the potential of reduction of the M(III)O_2^- adduct and not at the potential of the M(III)/(II) couple if adduct formation takes place before the transfer of an electron from the electrode. The latter should only be observed if the reaction were outer sphere, where O_2 would only collide with the redox center without the formation of a bond. In the special case of iron phthalocyanines and other macrocyclics, O_2 reduction usually starts at potentials very close to the Fe(III)/(II) couple [82, 102, 103]. In contrast, for cobalt macrocyclics reduction of O_2 begins at potentials much more negative than those corresponding to the Co(III)/(II) couple [14]. Several authors have reported correlations between activity (measured as potential at constant current) and the M(III)/(II) formal potential and volcano-shaped curves have been obtained [14, 15, 104, 105].

This could indicate that the redox potential needs to be located in an appropriate window to achieve maximum activity. In other words, a M(III)/(II) formal potential that is too negative (easily oxidable metal center) or a M(III)/(II) formal potential that is too positive (metal center that is more difficult to oxidize) does not favor the catalysis. However, more recent studies [94, 106–109] have shown that when comparing families of metallophthalocyanines, linear correlations are obtained when plotting log k or log I (rate constant or current at fixed potential) vs. the M(III)/(II) formal potential, as illustrated in Fig. 7.20. First-order rate constants were calculated as $k = I/nAFc$, where I is the current at a given potential, n is the total number of electrons transferred which is 2 for the peroxide pathway and 4 for the reduction to H_2O, A is the area in cm^2, F is the Faraday constant, and c is the oxygen concentration in moles per cm^3. One linear correlation is obtained for Cr, Mn, and Fe complexes and these metals have configurations d^4(Cr), d^5(Mn), and d^6(Fe). Another linear correlation is obtained for Co complexes, which have a configuration d^7. An interesting feature in the data of Fig. 7.20 is that the lines are parallel with a slope close to +0.15 V/decade. It is possible that the straight lines in Fig. 7.20 are part of an incomplete volcano correlation. If so, the slope 0.15 V/decade might have a physical meaning as discussed for the oxidation of thiols [110]. The data in Fig. 7.20 strongly suggest that more positive redox potentials will increase the catalytic activity, and it is good that no volcano correlation is obtained because there seems to be room for improving the catalytic activity of phthalocyanines or other macrocyclics. The M(III)/(II) redox potential of some macrocyclics can be shifted in the positive direction with heat treatment, and this could increase the catalytic activity. For example, when iron tetraphenylporphyrin [92], FeTPP, is heat treated, the Fe(III)/(II) redox transition is shifted from 0.2 V vs. RHE for fresh FeTPP to 0.4 V for FeTPP heat treated at 700 °C. Intermediate redox

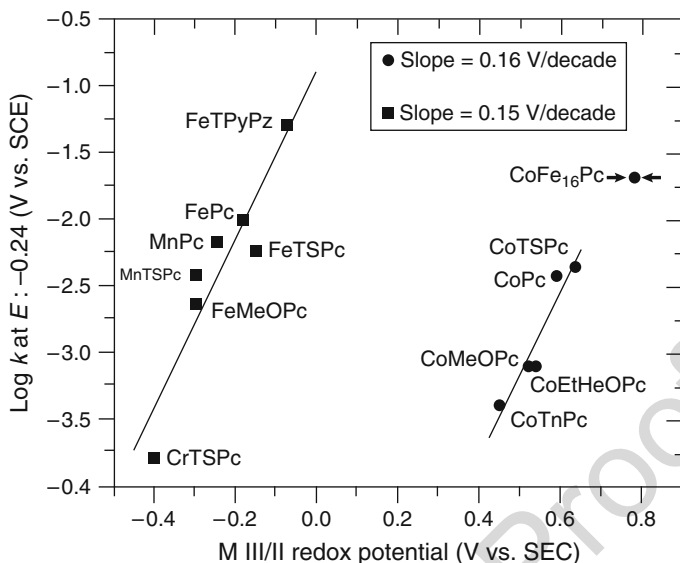**Fig. 7.20** Plot of log k (at constant potential vs. the M(III)/(II) formal potential of the MN_4 macrocyclic for the reduction of oxygen in 0.2 M NaOH) (from [106])

potentials are obtained for heat treatments at intermediate temperatures [92], and the catalytic activity increases with heat treatment, showing that a more positive redox potential of the catalyst favors the O_2 reduction reaction rate.

In a recent study [111], it has been discussed that the changes in the formal potential of the catalyst could explain the high catalytic activity of ORR that has been obtained by heat treatment of metallomacrocyclics and other starting materials. For example, when comparing data obtained with heat-treated catalysts prepared by very different techniques and starting materials, not necessarily involving metallomacrocyclic complexes [112], a correlation of log i (as currents normalized per mass of catalysts) vs. the formal potential of the catalyst gives what could be considered a linear correlation (see Fig. 7.21).

The scatter of the data could be attributed to differences in the porosity of the electrode prepared and also to differences in the number of active sites per unit of surface area. But in spite of this, a clear trend in the figure shows that more positive formal potentials seem to favor the catalytic activity of the different materials. Since the structures of the different catalysts used in the correlation of Fig. 7.21 are not known, no chemical formulas can be given and the numbers correspond exactly to those given in the original paper. More discussion on heat-treated materials will be given on other chapters of this book.

The increase in activity as the M(III)/(II) redox potential of the catalysts is more positive is in contrast to what was previously found in volcano correlations where a maximum activity is observed for intermediate redox potentials not only for the reduction of O_2 but for other reactions such as the oxidation of thiols or of hydrazine [99]. When studying a series of unsubstituted and substituted Mn phthalocyanines,

Fig. 7.21 Plot of log i_M (in Ag^{-1}) at $E = 0.8$ V vs. the formal potential of the catalyst for ORR [111, 112]
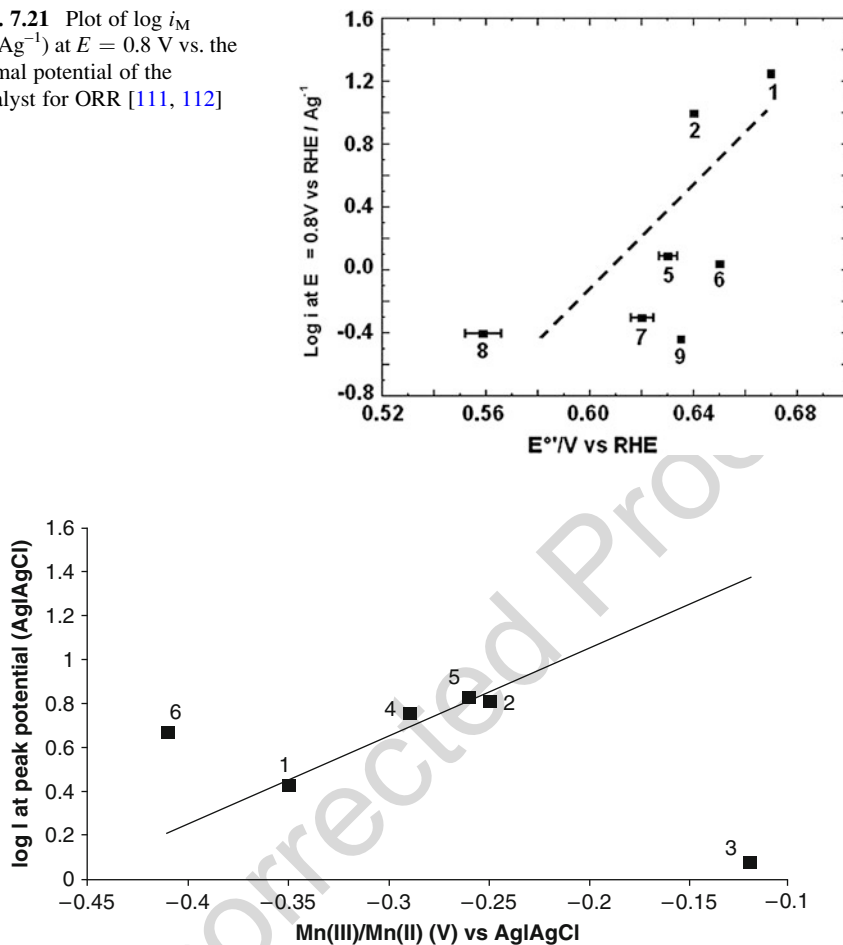

Fig. 7.22 Plot of log i vs. MnIII/MnII redox potential for oxygen reduction in pH 5 buffer. Manganese phthalocyanine (MnPc, 1), manganese tetraaminophthalocyanine (MnTAPc, 2), manganese tetrapentoxy pyrrole phthalocyanine (MnTPePyrPc, 3), manganese tetra phenoxy pyrrole phthalocyanine (MnTPPyrPc, 4), manganese tetra mercaptopyrimidine phthalocyanine (MnTMPyPc, 5), and manganese tetra ethoxy thiophene phthalocyanine (MnTETPc, 6) [109]

762 Nyokong and Sehlotho [109] have also found that the catalytic activity of these
763 complexes increases as the Mn(III)/(II) becomes more positive (see Fig. 7.22) with
764 a slope of 0.24 V/decade. It is very likely that the data in Figs. 7.20, 7.21, and 7.22
765 are part of an incomplete volcano and this is very important because it means that
766 hypothetically that catalysts with higher activities could be prepared by shifting the
767 formal potential to more positive values.

768   A possible explanation for the results in Fig. 7.22 (activity decreases as the driving
769 force of the catalyst increases) is that the electronic coupling between the donor
770 (MPc) and the acceptor (O_2) decreases as the electron-donating capacity of the

substituents increases, due to a shift in the energy of the frontier orbitals of the 771 metallophthalocyanine [113–115]. The shift in the energy of the frontier orbital 772 with substituents on cobalt phthalocyanines has been calculated by Schlettwein 773 [113] and Cárdenas-Jirón [116] using PM3 and ZINDO/S semiempirical theoretical 774 calculations. There are several approaches to estimate the electronic coupling matrix 775 elements between the donor and the acceptor in electron transfer reactions. One of 776 them considers the energy difference between the LUMO (lowest unoccupied molec- 777 ular orbital) of the electron acceptor and the HOMO (highest occupied molecular 778 orbital) of the electron donor [117] but this requires to know the distance that 779 separates the donor from the acceptor. This is not simple for an inner-sphere reaction 780 where the $M \cdots O_2$ distance could vary from complex to complex. To avoid this 781 difficulty, another reactivity index can be used to explain the data in Fig. 7.20 and 782 this is the concept of molecular hardness which is a commonly used criterion of 783 reactivity in organic reactions as proposed by Pearson [118, 119]. The hardness η of a 784 single molecule is approximately one-half the energy gap of the HOMO–LUMO, so 785 the larger the gap, the greater the hardness, the more stable the molecule (the harder 786 the molecule, the less its reactivity). The opposite corresponds to a molecule with a 787 narrow HOMO–LUMO gap (soft molecule) situation that will correspond to a very 788 reactive molecule. Now for a donor–acceptor pair, it is more convenient to use the 789 concept of donor–acceptor hardness η_{DA} which is one-half the difference between the 790 energy of the LUMO of the acceptor (O_2 molecule) and the energy of the HOMO of 791 the donor (metal complex): 792

$$\eta_{DA} = \frac{1}{2}\left(\varepsilon_{LUMO acceptor} - \varepsilon_{HOMO donor}\right) \tag{7.9}$$

The donor–acceptor intermolecular hardness can also be described as one-half 793 the difference between the ionization potential of the donor and the electron affinity 794 of the acceptor: 795

$$\eta_{DA} = -\frac{1}{2}\left(\varepsilon_{acceptor} - \varepsilon_{donor}\right) \tag{7.10}$$

For a gas phase reaction involving the transfer of a single electron, this will be 796 equivalent to the Gibbs free energy of the process ΔG°. For the special case of Co 797 phthalocyanine in its ground state, the HOMO is occupied with a single electron 798 (doublet state) so it corresponds to a single occupied molecular orbital (SOMO). 799 The same is valid for molecular oxygen, which in its ground state has two unpaired 800 electrons in two degenerate π^* antibonding orbitals. In this case, the formation of an 801 adduct CoPc-O_2 involves the interaction of two SOMOs and η_{DA} is given by 802

$$\eta_{DA} = \frac{1}{2}\left(\varepsilon_{SOMO acceptor} - \varepsilon_{SOMO donor}\right) \tag{7.11}$$

Figure 7.23 illustrates the calculated energy levels of the SOMOs of the different 803 cobalt phthalocyanines with respect to the SOMO of oxygen using PM3. 804

Fig. 7.23 (**a**) Relative
energies of frontier orbitals of
dioxygen and substituted Co
phthalocyanines. For
simplicity, only one electron
is shown on the SOMO of the
CoPcs [115]. (**b**) Plot of
log k (at constant potential)
vs. the donor–acceptor
intermolecular hardness for
the different O_2–CoPc pairs
(reproduced from [114])
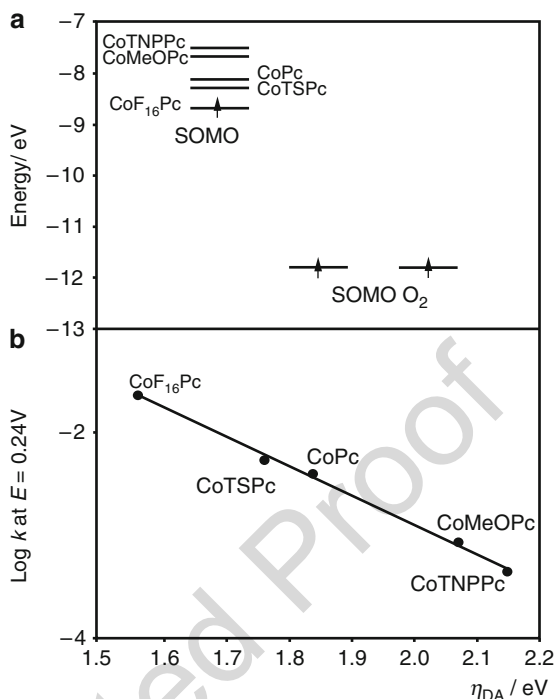
Electron-withdrawing substituents (sulfonate, fluoro) on the phthalocyanine ring
stabilize the SOMO and the opposite is true for electron-donating groups (methoxy
and neopentoxy). So electron-withdrawing groups, even though they decrease the
electron density on the cobalt (more positive redox potential), also decrease the gap
between the energy of the SOMO of the phthalocyanine and the energy of the
SOMO of oxygen. The bottom of Fig. 7.23 shows that log k for O_2 reduction
increases as the chemical hardness of the system decreases or as the softness of the
system increases (more reactivity). The trend in reactivity is exactly the same as
that illustrated in Fig. 7.20. It can be concluded then that hardness could be used as a
criterion for reactivity of these systems when comparing complexes that bear the
same structure and could explain why, for example, perfluorinated phthalocyanine,
which has the most positive redox potential (the most oxidant), is the best catalyst
for O_2 reduction in alkaline media in the series of cobalt phthalocyanines examined.

Quantum theories of elementary heterogeneous electron transfer (ET) reactions
in polar media have been extended to reactions which proceed through active
intermediate electronic surface band states or bands. On the basis of this theoretical
framework, Ulstrup [120] has interpreted experimental data obtained for O_2 reduc-
tion catalyzed by metal phthalocyanines.

When comparing activities of complexes by plotting constant potential vs. redox
potential of the catalyst, linear correlations are also obtained (see Fig. 7.24) and this
was predicted theoretically by the work of Ulstrup [120]. The slope of the lines in

Fig. 7.24 Plot of log E (at constant current) vs. the M(III)/(II) formal potential of the MN$_4$ macrocyclic for the reduction of oxygen in 0.2 M NaOH (from [106])
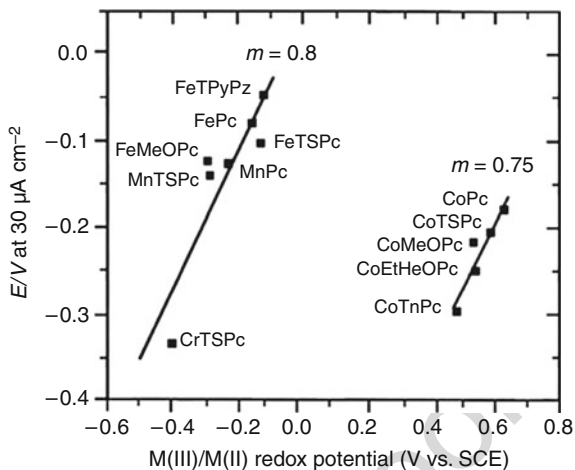

Fig. 7.24 is less than one, which was also predicted by Ulstrup and is attributed to the excitation of intramolecular modes of relatively low frequencies in the cathodic range. The data shown in Fig. 7.24 is essentially similar to that shown in Fig. 7.20 but the comparison was made at constant current. So essentially, the graph of Fig. 7.20 is a plot of driving force vs. driving force. This carries the assumption that the M(III)/(II) redox potential provides a measure of the driving force of the catalysts. Since catalysts produced by heat treatment, using MN$_4$ metal macrocyclics as the starting materials, or other ingredients like metal salts and nitrogen-containing compounds show very high activities and stabilities, especially in acidic media, it is interesting to compare activity parameters such as those in Fig. 7.20, that is, potential at constant current vs. the formal potential of the catalyst for this type of catalysts.

A correlation of this sort is illustrated in Fig. 7.25 [111] and includes catalysts reported by several groups in a joint article [112]. It is interesting to note that in spite of the scatter of the data, it seems that a linear correlation does exist, similar to that illustrated in Fig. 7.20. The slope is 1.2, which is not too far from unity as predicted by Ulstrup. If one compares the data in Fig. 7.21 with that in Fig. 7.25, the scatter of the data in Fig. 7.20 is much lower than that in Fig. 7.25 because it was obtained with graphite electrodes modified with monolayers of MN$_4$ macrocyclics. So the amount of active sites per unit of real area is very similar for all cases, which might not be true for the data in Fig. 7.25, in spite of the normalization of the current for the mass of catalysts per unit of geometric area. However, a trend is observed and again suggests that more positive formal potentials of the catalyst seem to favor the ORR catalytic process. Finally, it is important to point out that the formal potential plotted in Fig. 7.25 does not necessarily involve the M(III)/(II) but might involve metal-free redox functionalities generated after heat treatment as discussed in [112].

Not all metals of the first transition series exhibit the M(III)/(II) processes, so if one compares macrocyclics of different metals, it is convenient to use another parameter, for example, the number of d electrons in the metal as shown in
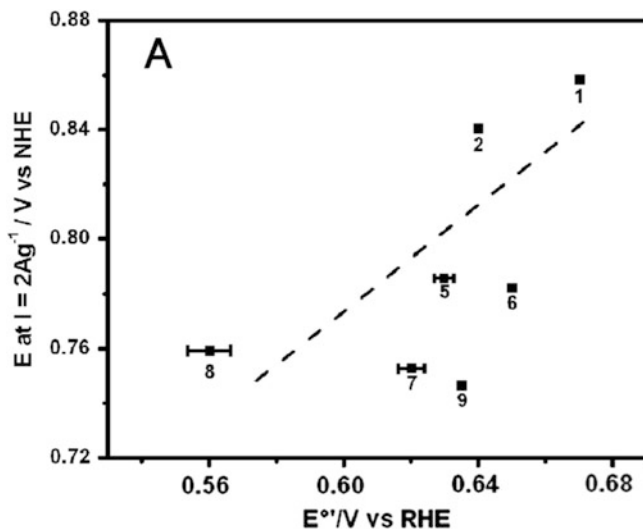
Fig. 7.25 Plot of log E (at constant current) vs. the formal potential of catalysts obtained by heat treatment for the reduction of oxygen in 0.05 M H_2SO_4 at 25 °C (reproduced by permission of the Electrochemical Soc [111], data from [112]). The labeling of catalysts is the same as that used in the original reference [112]

Fig. 7.26. In this figure, since different Tafel slopes are obtained for the different catalysts, it is not simple to compare activities as current at constant potential. So instead, as a criterion of activity, potential at constant currents is used.

Figure 7.26 clearly shows that Fe derivatives exhibit the highest activity, followed by Mn and Co and also illustrates a common observation in catalysis that metals with nearly half-filled d-energy levels exhibit the highest activity. So a redox type of mechanism does not operate for metals that do not exhibit the M(III)/(II) transition in the potential window examined for O_2 reduction. This is the case for Ni, Cu, and Zn phthalocyanines. It is important to point out that in order to have catalytic activity, the frontier orbital of the MN_4 needs to have some d character as illustrated in Fig. 7.16. The catalysts with higher activity included in Fig. 7.24 (Cr, Mn, Fe, Co) have frontier orbitals with d character, whereas in Ni and Cu phthalocyanines, the frontier orbitals have more ligand character [121]. This is illustrated in Fig. 7.27 [108] that compares the frontier orbitals of CoPc and CuPc. CoPc shows a well-defined dz^2 orbital sticking out of the plane of the phthalocyanine, whereas CuPc does not and shows low activity for O_2 reduction.

There is experimental evidence to support this using tunneling electron microscopy. It has been shown a strong d orbital dependence on the images of metal phthalocyanines (see Fig. 7.28).

Unlike copper phthalocyanine where the metal appears as a hole in the molecular image, cobalt phthalocyanine shows the highest point in the molecular image [122]. The benzene regions of CoPc and CuPc show the same height. So, essentially the

Fig. 7.26 Volcano plot for the electrocatalytic activity of different M-tetrasulfonated phthalocyanines adsorbed on graphite for O_2 reduction in 0.1 m NaOH, as a function of the number of d electrons in the metal (from [15])
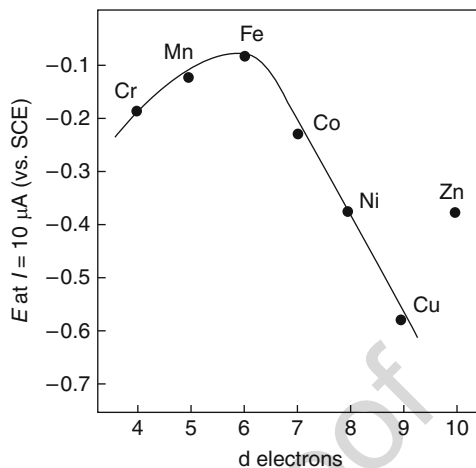
Fig. 7.27 Illustration of the frontier orbitals involved in the interaction of cobalt phthalocyanine with O_2 (reprinted from [108])
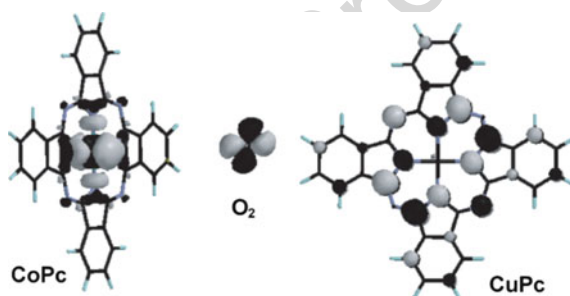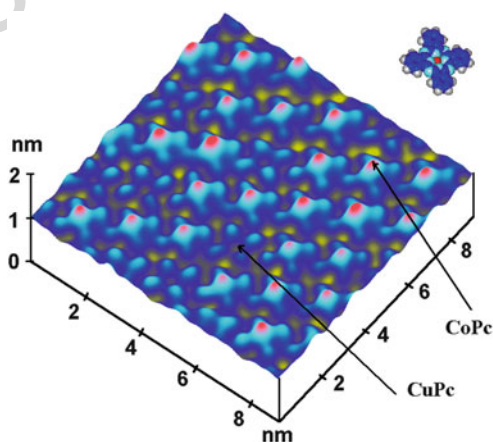

Fig. 7.28 STM surface plot image of CoPc and CuPc coadsorbed on the (111) plane of Au [122]

data using images generated using electron tunneling microscopy is in agreement 877
with the images generated by theoretical calculations. 878

Even though most authors agree that the M(II) state is the active site for O_2 879
reduction [15, 20, 65–67, 70, 72, 88, 89, 97–99, 102, 105, 123, 124] for FePc (iron 880
phthalocyanine) and FeNPc (iron naphthalocyanine) [125–127], it has been proposed 881

882 that Fe(I) could also play a role in the electrocatalytic process. This was based on
883 electroreflectance experiments that indicated that Fe(I) interacts with O_2 whereas Fe
884 (II) does not. However, many authors have shown experimental evidence that O_2
885 reduction commences at potentials much more positive than those corresponding to
886 the Fe(II)/(I) couple [14, 82, 97, 99]. On the contrary, the reduction currents are
887 observed at potentials close to the potential of the Fe(III)/(II) couple, so it seems
888 unlikely that Fe(I) could be the active site. Worse, as shown from rotating ring-disk
889 experiments, Fe(I) only favors the two-electron reduction in contrast to Fe(II)
890 [82, 88].

891   The catalytic activity can also depend on the amount of metal complex present on
892 the electrode surface. In general, the amount of catalyst present on the surface is
893 evaluated from cyclic voltammograms, measuring the electrical charge under revers-
894 ible peaks. This carries the assumption that all adsorbed catalyst gives an electro-
895 chemical signal. This might not necessarily be true and there could be a fraction of
896 complexes present on the surface that are electrochemically silent. It is assumed that
897 the "electroactive" adsorbed species are also active for the reduction of O_2.

898   It has been found that the O_2 reduction currents are directly proportional to the
899 amount of catalyst present [21, 128], when the catalysts is adsorbed on the electrode
900 surface indicating that the reaction is first order in the surface concentration of
901 catalyst. This is not true for cases where the catalyst is incorporated to the surface
902 by vapor deposition or when the catalyst is deposited from solutions and the solvent
903 is completely evaporated [21]. An explanation for these different observations is
904 that when the catalyst is deposited by vapor deposition or from complete evapora-
905 tion of solutions, multilayers are formed, and the metal active centers are not all
906 completely accessible to the O_2 molecule. Another example of this type of behavior
907 is the case for polymerized multilayers of cobalt tetraaminophthalocyanines, where
908 it has been demonstrated that only the outermost layer is active for the reduction of
909 O_2 [84, 85]. Scherson et al. [129] have reported that when $(FeTMPP)_2O$ is deposited
910 on a porous support, only 30 % of the amount deposited is found to be electro-
911 chemically active. Anson et al. [130] have found that for the case of $CoPc(CN)_{16}$
912 and $CoPcF_{16}$ that were deposited from solutions where the solvent was completely
913 evaporated, again it was found that only 30 % of the amount deposited was
914 electrochemically active. It was concluded that only those molecules that directly
915 exposed to the electrolyte and to the incoming O_2 molecules and at the same time
916 are in electric contact to the electrode are active for the reduction of O_2. These
917 results are not surprising since when multilayers are deposited, not all are necessar-
918 ily in electrical contact with the electrode, which is not the case for adsorbed layers,
919 where molecules are probably lying flat on the electrode surface, interacting with
920 the π system of the graphitic planes. Van der Putten et al. [131] have observed
921 catalytic activity with vacuum-deposited layers in spite of the fact that these layers
922 are electrochemically silent. As pointed out before when multilayers of metal
923 phthalocyanines are deposited on an electrode surface, only the outermost layer is
924 active for the reduction of O_2 [131] and this is also true for other electrochemical
925 reactions. This shows that multilayers of phthalocyanines or polymerized

multilayers of phthalocyanines are rather compact and the inner layers are not accessible to O_2 molecules [85].

7.3.1.2 N_4-Metallomacrocyclic Catalysts for One-Electron Reduction of O_2

An electrode surface that has no active sites should only promote the outer-sphere one-electron reduction of dioxygen. An example of such surface is a defect-free electrode surface that exposes the basal plane of graphite [124]. On the basal plane, all carbon atoms are fully coordinated so they cannot bind an oncoming molecule like O_2. On electrodes modified with adsorbed catalysts, to the best of our knowledge, there is only one report that shows evidence for the one-electron reduction of O_2 in alkaline media. A reversible one-electron reduction of O_2 to produce the stable superoxide ion was observed in an aqueous solution of 1 M NaOH. This electroreduction of O_2 was catalyzed by Cobalt(II) 1,2,3,4, 8,9,10,11, 15,16,17, 18,22,23,24,25-hexadecafluoro-29H,31H-phthalocyanine (abbreviated as $Co^{II}PcF_{16}$) adsorbed on a graphite electrode [132]. What is curious is that $Co^{II}PcF_{16}$ is the most active catalyst for the two-electron reduction of O_2 in the correlations shown in Figs. 7.17, 7.19, and 7.20, so it is very surprising that it can promote the one-electron reduction of O_2. The OH^- concentration has a very strong effect on the reduction process. Higher OH^- concentrations could stabilize the superoxide ion [124] but 1 M NaOH might not be concentrated enough to achieve this purpose so it could be interetsing to check this experiments by using electron paramagnetic resonance (EPR) techniques to detect any superoxide formation.

7.3.1.3 N_4-Metallomacrocyclic Catalysts for Two- and Four-Electron Reduction of O_2

Most mononuclear Co macrocyclics catalyze the reduction of dioxygen via two electrons to give peroxide [28, 82, 97, 99, 123]. The activity of Fe phthalocyanines in general is higher than those of Co phthalocyanines and the opposite is true for porphyrins, which reveals the importance of the nature of the ligand in determining the catalytic activity [96]. The opposite is true for heat-treated materials [133]. Cobalt complexes are more stable than iron complexes and this trend is maintained after heat treatment [72, 105]. However, iron complexes tend to promote the four-electron reduction of dioxygen and this will be discussed further on.

Lamy et al. [134] and van der Putten et al. [135] conducted spectroscopic investigations of polymer-modified electrodes containing CoTSPc using UV–visible differential reflectance spectroscopy and were able to identify Co(III)/Co(II) transition when varying the electrode potential. They used electron spin resonance on the Ppy (polypyrrole) and Ppy-CoTSPc electrodes in deoxygenated and oxygen-saturated solutions. It was shown that the Co(III)TSPc species is effective in the electroreduction of oxygen and that this species is more stable in oxygen-saturated medium than in deoxygenated medium because of its stabilization under the
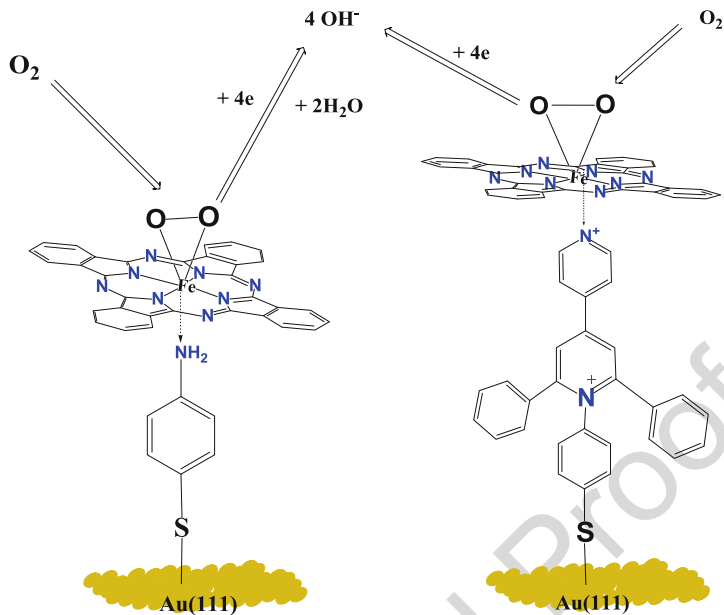
Fig. 7.29 Illustration of the catalytic action of FePc bound to gold via a self-assembled monolayer of axial ligand bound to Au [137]

965 following form: Co(III)–O_2. In the case of Ppy-CoTSPc film, the polypyrrole matrix
966 undergoes strong interactions with oxygen species and, most likely, with hydrogen
967 peroxide.

968   Phosphoric acid is one of the electrolytes used in fuel cells although very few
969 studies have focused attention on the activity of metallomacrocyclic complexes in
970 this electrolyte. Vasudevan and Phougat [136] investigated the electrocatalytic
971 activity of cobalt phthalocyanine monomers and polymers with imido and carbox-
972 ylic group ends. The complexes were mixed with carbon powder and polyethylene
973 powder. The activity of the monomeric compounds was found to be higher than that
974 of polymeric compounds.

975   However, in recent work, Ponce et al. [137] have shown that when Fe phthalo-
976 cyanine is anchored on gold via self-assembled axial ligands, the electrocatalytic
977 activity for ORR increases (see Fig. 7.29). The increase in activity seems to be
978 associated to the electron-withdrawing effect of the axial ligand. This will shift the
979 Fe(III)/(II) formal potential in the positive direction which favors the catalysis as
980 shown in Fig. 7.24.

981   When the catalytic activity of graphite modified with mixtures of different
982 proportions of FeTSPc and CoTSPc was tested for ORR, it was found that the
983 catalysts acted independently, that is, the amount of peroxide generated was directly
984 proportional to the fraction of CoTSPc present on the electrode surface. FeTSPc did
985 not promote the decomposition or reduction of peroxide generated on sites occupied
986 by CoTSPc. However, the possibility for the Fe centers to form hydrogen peroxide

and promote its decomposition cannot be ruled out completely since Fe(II) sites are known for their catalase activity [138]. Indeed for some metal complexes van Veen et al. have found that their catalytic activity for peroxide decomposition is directly proportional to its activity for O_2 reduction [139].
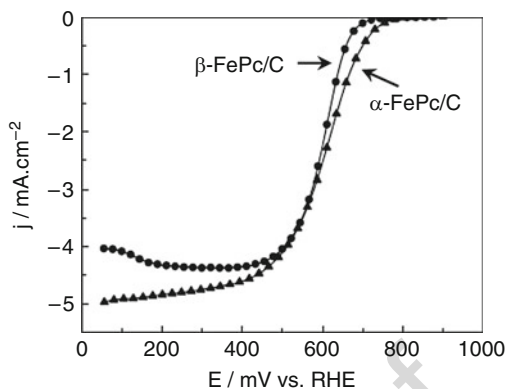
Again, as observed with FeTSPc and FePc [77, 87, 140, 141], a prewave is observed for the reduction currents and corresponding to the direct four-electron reduction. In contrast to FeTSPc or FePc, production of peroxide was attributed to reduction of the ligand and not reduction of the metal (Fe(I) formation). For this particular catalyst, it was suggested that dioxygen can bind to the Fe center and to a highly electronegative nitrogen in the ring, which will avoid the desorption of peroxide before it is reduced. This dual-site mechanism would aid charge injection via backbonding from the macrocycle into antibonding orbitals of O_2 or bound peroxide causing the destabilization and further rupture of the O–O bond [142]. At more negative potentials at which reduction of the ligand takes place, this mechanism becomes inoperative, the O_2 molecule only binds to the Fe center, and peroxide can desorb into the solution. In a study involving heat-treated FeTPP [143] and deposited by thick layers on glassy carbon, it was found that the amount of hydrogen peroxide decomposed, compared to the amount of oxygen and hydrogen peroxide reduced, was so small that chemical decompositions were ruled out.

Van den Brink et al. [141] when using vacuum-deposited layers of FePc have found that when examining the catalytic activity of these layers, the first reduction wave scan was very different from subsequent scans, indicating that some reorganization of the deposited layers took place since this phenomenon is not observed on adsorbed layers of FePc. The effect of irreversible changes of FePc when treated under potential load with oxygen is only observed using vacuum-deposited multilayers [125]. Léger et al. pointed out that the structure of FePc films influences their electrocatalytic activity.

XRD studies have shown that non-heat-treated FePc is under the α-phase whereas heat-treated FePc is under the β-phase. Surprisingly, the α-phase shows higher activity than the β-phase (see Fig. 7.30). These authors have also shown using electrochemical quartz crystal microbalance (EQCM) that α-phase FePc probably forms μ-oxo dimers at potentials higher than 700 mV vs. RHE. These μ-oxo dimmers are reduced at the same potential than the monomer of α-phase FePc [142].

Theoretical studies performed by Anderson and Sidik [144] using spin-unrestricted hybrid gradient-corrected density functional calculations have predicted that Fe(II) is the active site for four-electron reduction of oxygen by iron in the N_4Fe systems employed in the calculation, and it may be suggested that the same should be expected for heat-treated iron macrocyclics. The calculations have shown that Fe(II) is favored over Fe(III) because H_2O bonds strongly to the Fe(III) site, preventing O_2 adsorption and water does not bond strongly to Fe(II). On a first step, –OOH bonds more strongly to Fe(II) than to Fe(III), which results in a calculated more reversible potential for its formation over Fe(II). Calculations show that subsequent reduction steps have very reversible potentials over both centers (Fe(II) or Fe(III)). Calculations also show a hydrogen bonding interaction between –(OHOH) bonded to Fe(II) and to a nitrogen lone-pair orbital in the N_4 chelate. This interaction prevents peroxide from

Fig. 7.30 Polarization curves for the oxygen reduction on a α-FePc/C (m) and a β-FePc (d) disk electrode recorded at 2,500 rpm in O_2-saturated 0.5 M H_2SO_4 electrolyte ($T = 20\,^{\circ}C$, $v = 5\,mV\,s^{-1}$) [142]
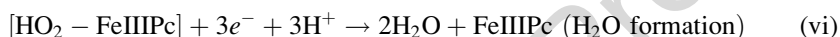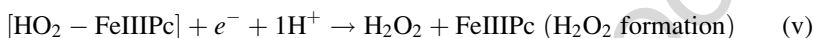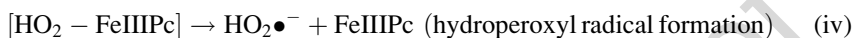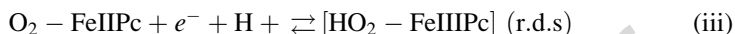
desorbing as a two-electron reduction product. So essentially these studies show that adsorbed hydrogen peroxide in an intermediate formed from N_4Fe–OOH on Fe(II) sites and can be released into the solution at more negative potentials as found experimentally [14, 28].

Most catalysts investigated usually have Fe and Co as metal centers. However, complexes of other metals have also been studied. For example, CrTSPc and MnTSPc exhibit catalytic activity for ORR [14] and they somehow resemble the behavior of Fe complexes, especially MnTSPc, in the sense that it shows a prewave where O_2 reduction proceeds entirely via four electrons to give water. Peroxide is produced at higher polarizations. The lower activity of Cr and Mn phthalocyanines compared to Fe phthalocyanines can be attributed to their low redox potential, that is, they are easily oxidized [82, 105]. The activity of most macrocyclic metal complexes increases after heat treatment [145]. However, the opposite is observed for manganese complexes probably because the metal is lost from the N_4 structure. So, most work dealing with heat-treated materials has focused on Fe and Co macrocycles. Complexes of Mo can only be used in alkaline solution since they are not stable in acid media. MoNPc is less activity than FeNPc as reported by Magner [146].

Very few authors have studied the effect of temperature [147] on the catalytic activity of phthalocyanines. Baker et al. [147] carried out experiments at different temeperatures in an acidic electrolyte to simulate the environment of an operating PEM fuel cell. They conducted experiments in the temperature range of 20–80 °C and using unsubstituted and substituted Fe phthalocyanines. The surface electro-chemical responses of the FePc species were characterized with respect to their surface concentrations and adsorbed surface orientations. Depending on the type of substituent, the adsorption mode could be flat, edge-on, as a dimer, or as an agglomerate, suggesting that the substituent has a strong effect on the FePc species' adsorption mode. Substitution also has a significant effect on stability. With respect to their electrocatalytic activity, both temperature, substitution, and possibly mode of adsorption can significantly affect the ORR mechanism. For example, the overall electron transfer number observed can change from 1 to 3 depending on the type of

substituent and the reaction temperature. Further research is required to determine if this change in *n* reflects a change in the ORR pathway and/or a decrease in the stability of the adsorbed ORR intermediates. Based on the various approaches found in the literature and the current understanding, a mechanism for the FePc species catalyzed ORR was suggested as follows:

$$FeIIIPc + e^- \rightleftarrows FeIIPc \tag{i}$$

$$FeIIPc + O_2 \rightleftarrows O_2 - FeIIPc \tag{ii}$$

$$O_2 - FeIIPc + e^- + H + \rightleftarrows [HO_2 - FeIIIPc] \ (r.d.s) \tag{iii}$$

$$[HO_2 - FeIIIPc] \rightarrow HO_2\bullet^- + FeIIIPc \ (hydroperoxyl \ radical \ formation) \tag{iv}$$

$$[HO_2 - FeIIIPc] + e^- + 1H^+ \rightarrow H_2O_2 + FeIIIPc \ (H_2O_2 \ formation) \tag{v}$$

$$[HO_2 - FeIIIPc] + 3e^- + 3H^+ \rightarrow 2H_2O + FeIIIPc \ (H_2O \ formation) \tag{vi}$$

It is worth mentioning that Wilkinson et al. [148] have also conducted studies at different temperatures using Fe fluoroporphyrin and reported some kinetic parameters such as activation energies. They found that the results were essentially similar to those found with FePc.

7.4 Oxygen Reduction Catalyzed by Nonmacrocyclic Cu Complexes

Copper (I) complexes exhibit catalytic activity for the four-electron (4-e) reduction of O_2 to water. Natural occurring enzymes like Cu-containing fungal laccase reduce O_2 directly to water very efficiently at very positive potentials, not far from the thermodynamic standard potential of the O_2/H_2O couple. These enzymes involve a trinuclear Cu active site [149–153]. For this reason some authors have investigated the catalytic activity of Cu(I) complexes for ORR, in particular Cu phenanthrolines confined on graphite or glassy carbon surfaces [154–169], with the aim of achieving the total reduction of O_2 via the transfer of four-electrons.

For example, copper(I) 1,10-phenanthroline, Cu(phenP), reduces O_2 almost entirely via the transfer of four electrons and four protons to give water [156, 157, 170]. This is quite interesting since, similarly to what is observed with Fe phthalocyanines [99, 171], the four-electron reduction of O_2 is promoted by single-site catalysts. The O_2 molecule cannot interact simultaneously with two Cu active sites. If this were the case, the order of the reaction in surface concentration would equal to two. Anson et al. [156, 157, 170] checked this and found that the reaction is first order in Cu coverage, suggesting of a mononuclear Cu site as the active

1090 catalyst. As mentioned above, Cu-containing fungal laccase enzymes promote the
1091 reduction of molecular oxygen directly to water at a trinuclear Cu active site at very
1092 low overpotentials [149, 150]. Using specially designed laccase-modified
1093 electrodes, Heller et al. [172–174] have measured current densities of 5 mA/cm^2
1094 at overpotentials (vs. the O_2/H_2O couple) as low as -0.070 V at pH 5. As discussed
1095 by Chidsey et al. [168], this current density corresponds to a turnover rate of 2.1 O_2
1096 reduced per laccase s^{-1}, or 0.7 O_2 per Cu s^{-1}. In comparison, as pointed out by
1097 Chidsey et al. [168], Pt nanoparticle catalysts reduce O_2 with rates of 2.5 O_2 per
1098 active surface Pt s^{-1} or 0.25 O_2 per total Pt s^{-1}, at an overpotential of -0.350 V
1099 [168, 175]. This normalization allows the comparison of atom efficiency of the
1100 catalysts regardless of catalyst loading [166]. With this evidence it is possible to
1101 design and prepare Cu complexes that can mimic enzymatic systems using mono-
1102 nuclear Cu complexes.
1103   Anson et al. found that 1,10-phenanthroline (phen) complexes of Cu, adsorbed
1104 on the edge-plane orientation of graphite, catalyze the four-electron reduction of O_2
1105 to H_2O [156–159, 170]. They proposed a mechanism for the electrocatalytic four-
1106 electron reduction of O_2. Using complexes having three different phen ligands
1107 (phen, 2,9-Me2-phen, 5-Cl-phen), they found that reduction of O_2 occurs at
1108 potentials negative to the formal Cu (II/I) redox potential of the respective complex
1109 strongly suggesting that the active species is the Cu(I) complex [158]. They
1110 conducted their studies in the presence of buffers containing acetate, phosphate,
1111 and borate. However, the mechanism proposed did not involve the coordination of
1112 these anions to the Cu center, even though these anions can affect the potentials and
1113 electrocatalytic activity of similar complexes [174]. Chidsey et al. [168] conducted
1114 a systematic study of the catalytic activity of several Cuphen complexes for ORR in
1115 the presence of acetate. They found that the reduction of Cu(II) on the adsorbed
1116 complexes occurs with the concerted dissociation of an acetate ion as [phenCu(II)
1117 AcO$^-$]$_{ad}$ + e^- > [phenCu(I)]$_{ad}$ + AcO$^-$ and that this can happen with any
1118 coordinating anion. They found that catalytic currents are observed at potentials
1119 very close to the Cu(II)/(I) formal potential of the adsorbed Cu phen complex. This
1120 is illustrated in Fig. 7.31. They found that the presence of the anion is crucial in the
1121 stability of the catalyst since irreversible degradation of the catalyst is observed if
1122 an O_2 reduction experiment is conducted in the absence of acetic acid. The effect of
1123 the $E^{\circ\prime}$, the Cu(II)/(I) formal of the catalyst on the ORR activity was studied by
1124 investigating some complexes with electron-withdrawing groups located on the
1125 phenanthroline ligand as illustrated in Fig. 7.31. As expected, these groups,
1126 according to their electron-withdrawing power, shift the Cu(II)/(I) formal potential
1127 to more positive values, as seen by the shift of the reversible waves (dotted lines) in
1128 Fig. 7.31 assigned to the Cu(II)/(I) transition.
1129   The shift to more positive potential of the Cu(II)/(I) formal potential has a
1130 positive effect in the catalytic activity of the complexes since the ORR waves
1131 (solid lines) also shift in the same direction, that is, to lower ORR overpotentials.
1132 Figure 7.32 illustrates the effect of the formal potential on the catalytic currents.
1133 The currents were measured at the formal potential of each catalyst, not at a
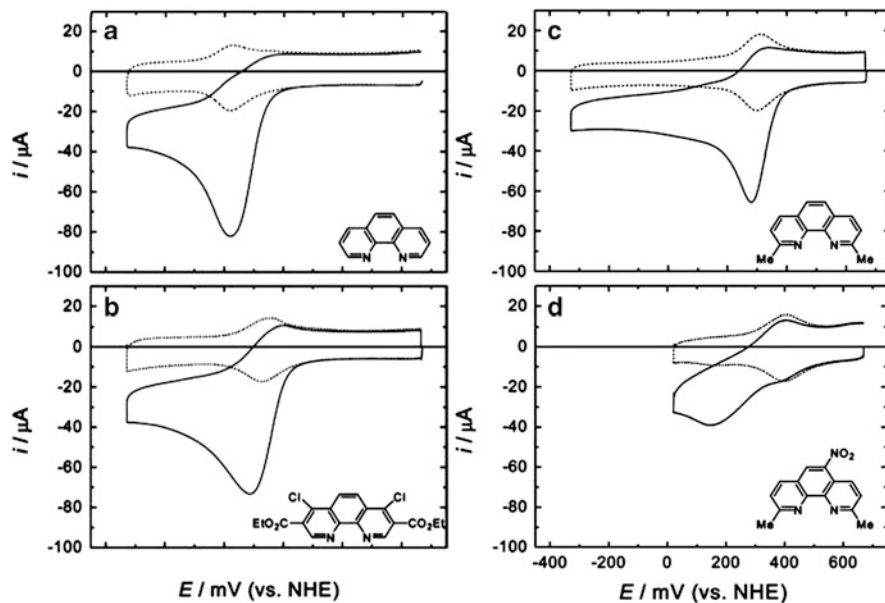1134 constant potential, and they are normalized for the amount of catalyst present on

Fig. 7.31 Cyclic voltammograms of edge-plane graphite modified with adsorbed Cu complexes of (**a**) phen, (**b**) 3,8-$(CO_2Et)_2$-4,7-Cl_2-phen, (**c**) 2,9-Me_2-phen, and (**d**) 2,9-Me_2-5-NO_2-phen, in N_2-purged (*dotted lines*) and air-saturated (*continuous lines*) solutions of 0.1 M $NaClO_4$, 0.020 M NaAcO, 0.02 M AcOH, pH 4.8 at 0.1 V s^{-1} as reported by Chidsey et al. [168]
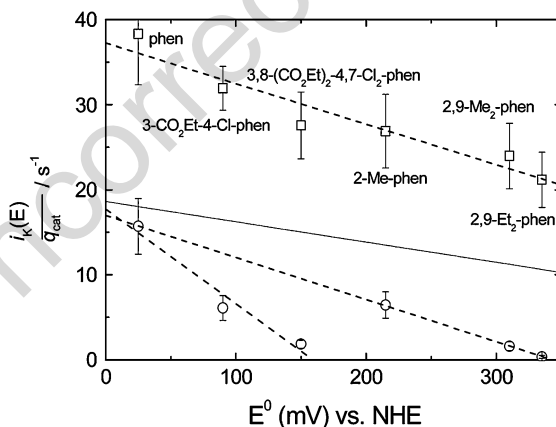

Fig. 7.32 Normalized kinetic currents for Cu complexes adsorbed on the edge-plane of graphite, measured at $E^{\circ\prime}$ (*circles*) and at -0.150 V vs. NHE (*squares*) plotted vs. $E^{\circ\prime}$ for each Cu complex. The *dotted line* is the expected behavior for the kinetic current measured at $E_{1/2}$. All data measured in 0.020 M NaAcO and 0.020 M AcOH pH 4.8, 0.1 M $NaClO_4$ except 2,9-Me_2-phen measured in 0.020 M NaAcO and 0.072 M AcOH pH 4.2, 0.1 M $NaClO_4$
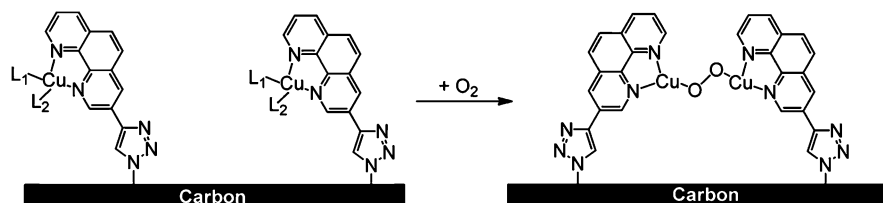
Fig. 7.33 Binding of dioxygen to two proximal Cu centers of 3-ethynyl-phenanthroline cova-lently attached to an azide-modified glassy carbon electrode according to Chidsey et al. [169]

the surface (the amount of catalyst is proportional to the electrical charge under the reversible peaks, dashed lines, in Fig. 7.31). It could be interesting to compare the currents at constant electrode potential vs. the formal potentials since it would be likely that a similar correlation to that shown in Fig. 7.20 illustrated for ORR on metallophthalocyanines vs. the M(III)/(II) formal potential, judging from the data in Fig. 7.31.

Chidsey et al. [169] have also studied the catalytic activity of a Cu(I) complex of 3-ethynyl-phenanthroline covalently attached to an azide-modified glassy carbon electrode. This catalyst promotes the four-electron reduction of O_2 at pH 4.8 (acetate buffer). In contrast to what is observed by Anson et al. [156–158, 170] using Cu phenanthroline, Chidsey et al. found a second-order dependence of the rates on Cu coverage at moderate overpotentials. This suggests that O_2 interacts with two Cu centers simultaneously, forming a bridge structure, as illustrated in Fig. 7.33.

Copper(I) complexes confined on electrode surfaces are promising catalyst for the four-electron ORR and seem to require the presence of coordinating anions like acetate to stabilize the adsorbed. This is a much less explored field of nonprecious metal catalysts compared to MN_4 macrocyclics for ORR and might be interesting to mimic laccase-like structures as this particular enzyme catalyzes the reduction of O_2 at very low overpotentials [151].

7.5   Conclusions

It can be concluded that in spite of the rather large amount of work published in the literature, there are still many questions that remain unsolved about the electrocatalytic reduction of O_2 mediated by N_4-metallomacrocyclics confined on electrode surfaces. Improving the activity of these complexes beyond the present state-of-the-art catalysts will require development of rigorous qualitative and quanti-tative structure–activity relationships (QSAR) [176] for judicious tailoring of activity. Some useful trends do exist. For example, it is now well established that Fe and Co macrocyclic complexes are by far the best catalysts for oxygen reduction even though some studies have demonstrated that cofacial Ir complexes are also very active. These complexes are characterized by exhibiting a reversible redox transition involving the M(III)/(II) couple. Some authors have found volcano-shaped correlations between activity (measured as current at constant potential or potential at constant current) vs.

M(III)/(II) formal potential of the catalyst suggesting that an optimal M(III)/(II) redox potential does exist for maximum activity. However, other authors have found only linear correlations between activity and M(III)/(II) redox potential, which indicates that the more positive the redox potential, the higher the activity. In the latter correlations, the activity decreases with increasing the driving force of the catalyst. This finding is important since a priori one would expect that the more negative the M(III)/(II) formal potential, the higher the activity, since this could favor the partial reduction of O_2 upon interacting with the metal center, that is, M(III)-O_2-. It is also possible that the linear correlations found are part of an incomplete volcano. However, in these correlations it was found that Cr, Mn, Fe, and Co complexes, which exhibit a M(III)/(II) transition, give rise to two separated correlations or families of compounds. This is a reflection of the fact that the reduction wave for O_2 reduction on, for example, Mn and Fe complexes starts at a potential very close to the M(III)/(II) formal potential of the catalyst. In contrast, for Co macrocyclics, the reduction wave starts at potentials far more negative than the Co(III)/(II) formal potentials. The proximity of the O_2 reduction wave to the M(III)/(II) for some complexes is also reflected in the observation that a direct four-electron reduction process operates, as observed for Fe and Mn complexes. For most monomeric or monolayers of Co complexes, the onset for O_2 reduction is far removed from the Co(III/II) transition and only the peroxide pathway is observed.

Biomimetic catalyst design schemes have been very successful in tailoring the properties of catalysts, for example, as demonstrated for functional heme/Cu analogs and bimetallic cofacial diporphyrins. The knowledge gained thus far provides a promising leeway for the design of efficient N_4-metallomacrocyclic based catalysts for four-electron reduction of oxygen.

Despite Ir- and Ru-based N_4-metallomacrocyclic complexes reporting some of the best activities in acidic and alkaline media, respectively, being rare metals, their advantageous superiority would be offset by their high cost. Nonetheless, these complexes should serve as appropriate models, such that theoretical and experimental knowledge gained from studying them may serve to tailor the synthesis of improved catalysts. Particularly, the energetic aspects that furnish some monomeric complexes the unique ability to reduce oxygen directly to water as opposed to other monomeric complexes warrant detailed investigation.

The relative backdonating power of metal ions attached to the pendant groups of the multinuclear oxygen reduction catalysts discussed in this work is the fundamental parameter for modulating the ORR activity of these complexes. It is therefore possible that the electronic effects introduced due to π backdonation by Ru(II) and Os(II) may also be fulfilled by other groups. This rationale constitutes the prospect for modulation of the ORR activity of these complexes.

The stability of metalloporphyrins and metallophthalocyanines alike is far from satisfactory for any practical application. Whereas there is irrefutable evidence for improved activity upon heat treatment of the N_4-metallomacrocyclic complexes, the loss of their structural merit is obvious. The fact that the performance of nonprecious metal catalysts synthesized by heat treatment of inexpensive nitrogen, carbon, and metal precursors rivals that of heat-treated N_4-metallomacrocyclic complexes, which

are relatively more expensive, renders the latter to be noncompetitive precursors [177]. On the other hand, improving the stability and activity of N$_4$-metallomacrocyclic complexes while conserving their molecular integrity is a difficult task, and indeed very little progress has been reported in line with this.

New material design approaches including exploitation of the synergetic benefits reported for some catalyst supports, for example, carbon nanotubes, graphene, nitrogen-doped carbons, and titanium oxide [178, 179] and other conductive mesoporous materials with high surface areas, among others, might help to solve some of the current challenges. The multicomponent and multifunctional approach [78, 180, 181], where the individual components of a composite catalyst perform specific reactions to ensure complete reduction of oxygen, is worthwhile engendering.

Finally, it is worth mentioning that one of the advantages of MN$_4$ macrocyclics over Pt catalysts is their tolerance to methanol crossover [14], which is a serious problem in methanol-air fuel cells [83]. For example, Léger et al. have shown that FePc is highly tolerant to methanol [182]. The same is true for CoPc [183]. When methanol crossover from the anode through the electrolytic membrane to the cathode occurs, electroreduction of dioxygen and electrooxidation of methanol occur simultaneously, which is detrimental to the overall performance of the fuel cell since the fuel efficiency decreases and so does the power output. In general MN$_4$ macrocyclics are poor catalysts for the oxidation of methanol so this reaction should not occur and this would avoid the problems mentioned above.

Cu(I) complexes that somehow mimic natural-occuring laccase represent an interesting class of catalysts since they catalyze the four-electron reduction of O$_2$ directly to water at rather low overpotentials at pH 4.8 but they lack long-term stability. However, it might be possible to solve this problem in the future.

References

1. Steele BC, Heinzel A (2001) Materials for fuel-cell technologies. Nature 414(6861):345–352
2. Lee J, Kim ST, Cao R, Choi N, Liu M, Lee KT, Cho J (2011) Metal-air batteries with high energy density: Li–Air versus Zn–Air. Adv Energy Mater 1(1):34–50
3. Gasteiger HA, Kocha SS, Sompalli B, Wagner FT (2005) Activity benchmarks and requirements for Pt, Pt-alloy, and non-Pt oxygen reduction catalysts for PEMFCs. Appl Catal B Environ 56(1–2):9–35
4. Spendelow JS, Wieckowski A (2007) Electrocatalysis of oxygen reduction and small alcohol oxidation in alkaline media. Phys Chem Chem Phys 9(21):2654–2675
5. Min M (2000) Particle size and alloying effects of Pt-based alloy catalysts for fuel cell applications. Electrochim Acta 45(25–26):4211–4217
6. Mazumder V, Lee Y, Sun S (2010) Recent development of active nanoparticle catalysts for fuel cell reactions. Adv Funct Mater 20(8):1224–1231

7. Sun Z, Masa J, Liu Z, Schuhmann MM (2012) Highly concentrated aqueous dispersions of graphene exfoliated by sodium taurodeoxycholate: dispersion behavior and potential application as a catalyst support for the oxygen-reduction reaction. Chem Eur J 18:6972–6978

8. Jasinski R (1964) New fuel cell cathode catalyst. Nature 201(492):1212–1213

9. Jahnke H, Schönborn M, Zimmermann G (1976) Organic dyestuffs as catalysts for fuel cells. In: Schäfer F, Gerischer H, Willig F, Meier H, Jahnke H, Schönborn M, Zimmermann G (eds) Physical and chemical applications of dyestuffs, vol 61. Springer, Heidelberg, pp 133–181

10. Alt H, Binder H, Sandstede G (1973) Mechanism of the electrocatalytic reduction of oxygen on metal chelates. J Catal 28(1):8–19

11. Kadish K (1984) Redox tuning of metalloporphyrin reactivity. J Electroanal Chem 168(1–2):261–274

12. Randin J (1974) Interpretation of the relative electrochemical activity of various metal phthalocyanines for the oxygen reduction reaction. Electrochim Acta 19(2):83–85

13. Richards G, Swavey S (2009) Electrooxidation of Fe, Co, Ni and Cu metalloporphyrins on edge-plane pyrolytic graphite electrodes and their electrocatalytic ability towards the reduction of molecular oxygen in acidic media. Eur J Inorg Chem 35:5367–5376

14. Zagal JH, Páez M, Tanaka A, dos Santos Jr JR, Linkous CA (1992) Electrocatalytic activity of metal phthalocyanines for oxygen reduction. J Electroanal Chem 339(1–2):13–30

15. Vasudevan P, Santosh MN, Tyagi S (1990) Transition metal complexes of porphyrins and phthalocyanines as electrocatalysts for dioxygen reduction. Transit Met Chem 15(2):81–90

16. Yuasa M, Nishihara R, Shi C, Anson FC (2001) A comparison of several meso-tetraalkyl cobalt porphyrins as catalysts for the electroreduction of dioxygen. Polym Adv Technol 12(3–4):266–270

17. Song E, Shi C, Anson FC (1998) Comparison of the behavior of several cobalt porphyrins as electrocatalysts for the reduction of O_2 at graphite electrodes. Langmuir 14(15):4315–4321

18. Ozer D, Harth R, Mor U, Bettelheim A (1989) Electrochemistry of various substituted aminophenyl iron porphyrins: Part II. Catalytic reduction of dioxygen by electropolymerized films. J Electroanal Chem 266(1):109–123

19. Bettelheim A, Ozer D, Harth R, Murray RW (1989) Electrochemistry of various substituted aminophenyl iron porphyrins: Part I. Redox properties of dissolved, adsorbed and electropolymerized species. J Electroanal Chem 266(1):93–108

20. van der Putten A, Elzing A, Visscher W, Barendrecht E (1987) Redox potential and electrocatalysis of O_2 reduction on transition metal chelates. J Electroanal Chem 221(1–2):95–104

21. Elzing A, van der Putten A, Visscher W, Barendrecht E (1986) The cathodic reduction of oxygen at cobalt phthalocyanine. Influence of electrode preparation on electrocatalysis. J Electroanal Chem 200(1–2):313–322

22. Beletskaya I, Tyurin VS, Tsivadze AY, Guilard R, Stern C (2009) Supramolecular chemistry of metalloporphyrins. Chem Rev 109(5):1659–1713

23. Tashiro K, Aida T (2007) Metalloporphyrin hosts for supramolecular chemistry of fullerenes. Chem Soc Rev 36(2):189

24. Sun D, Tham FS, Reed CA, Chaker L, Boyd PD (2002) Supramolecular fullerene-porphyrin chemistry. fullerene complexation by metalated "Jaws Porphyrin" Hosts. J Am Chem Soc 124(23):6604–6612

25. NEC (2007) Advanced energy initiative, 2006. National Environmental Council for the President of the United States

26. Adzic R (1998) Recent advances in kinetics of oxygen reduction. In: Lipkowski J, Ross PN (eds) Electrocatalysis. Wiley-VCH, New York, NY, pp 197–237

27. Bard AJ, Faulkner LR (2001) Electrochemical methods. Fundamentals and applications, 2nd edn. Wiley, New York, NY

28. Zagal JH, Bindra P, Yeager E (1980) A mechanistic study of O_2 reduction on water soluble phthalocyanines adsorbed on graphite electrodes. J Electrochem Soc 127(7):1506

29. Paulus UA, Schmidt TJ, Gasteiger HA, Behm RJ (2001) Oxygen reduction on a high-surface area Pt/Vulcan carbon catalyst: a thin-film rotating ring-disk electrode study. J Electroanal Chem 495(2):134–145

30. Dobrzeniecka A, Zeradjanin A, Masa J, Puschhof A, Stroka J, Kulesza PJ, Schuhmann W (2012) Application of SECM in tracing of hydrogen peroxide at multicomponent non-noble electrocatalyst films for the oxygen reduction reaction. Catal Today. doi:1016/j. cattod.2012.03.060

31. Okunola AO, Nagaiah TC, Chen X, Eckhard K, Schuhmann BM (2009) Visualization of local electrocatalytic activity of metalloporphyrins towards oxygen reduction by means of redox competition scanning electrochemical microscopy (RC-SECM). Electrochim Acta 54(22):4971–4978

32. Sánchez-Sánchez CM, Bard AJ (2009) Hydrogen peroxide production in the oxygen reduction reaction at different electrocatalysts as quantified by scanning electrochemical microscopy. Anal Chem 81(19):8094–8100

33. Mezour MA, Cornut R, Hussien EM, Morin M, Mauzeroll J (2010) Detection of hydrogen peroxide produced during the oxygen reduction reaction at self-assembled thiol − porphyrin monolayers on gold using SECM and nanoelectrodes. Langmuir 26(15):13000–13006

34. Sánchez-Sánchez CM, Rodríguez-López J, Bard AJ (2008) Scanning electrochemical microscopy. 60. Quantitative calibration of the SECM substrate generation/tip collection mode and its use for the study of the oxygen reduction mechanism. Anal Chem 80(9):3254–3260

35. Collman J, Ghosh S (2010) Recent applications of a synthetic model of cytochrome c. Inorg Chem 49(13):5798–5810

36. Kim E, Chufán EE, Kamaraj K, Karlin KD (2004) Synthetic models for heme − copper oxidases. Chem Rev 104(2):1077–1134

37. Collman J, Boulatov R, Sunderland CJ, Fu L (2004) Functional analogues of Cytochrome c oxidase, myoglobin, and hemoglobin. Chem Rev 104(2):561–588

38. Collman J, Devaraj NK, Decreau RA, Yang Y, Yan Y, Ebina W, Eberspacher TA, Chidsey CED (2007) A Cytochrome c oxidase model catalyzes oxygen to water reduction under rate-limiting electron flux. Science 315(5818):1565–1568

39. Boulatov R, Collman J, Shiryaeva IM, Sunderland CJ (2002) Functional analogues of the dioxygen reduction site in cytochrome oxidase: mechanistic aspects and possible effects of CuB. J Am Chem Soc 124(40):11923–11935

40. Chang CJ, Deng YQ, Shi CN, Chang CK, Anson FC, Nocera DG (2000) Electrocatalytic four-electron reduction of oxygen to water by a highly flexible cofacial cobalt bisporphyrin. Chem Commun 15:1355–1356

41. Collman J (1997) A functional model related to Cytochrome c oxidase and its electrocatalytic four-electron reduction of O_2. Science 275(5302):949–951

42. Collman J, Elliott CM, Halbert TR, Tovrog BS (1977) Synthesis and characterization of "face-to-face" porphyrins (biometallic ligands/metal-metal interactions/electron spin resonance/dioxygen reduction/dinitrogen reduction). Proc Natl Acad Sci U S A 74(1):18–22

43. Collman J, Denisevich P, Konai Y, Marrocco M, Koval C, Anson FC (1980) Electrode catalysis of the four-electron reduction of oxygen to water by dicobalt face-to-face porphyrins. J Am Chem Soc 102(19):6027–6036

44. Shigehara K, Anson FC (1982) Electrocatalytic activity of three iron porphyrins in the reduction of dioxygen and hydrogen peroxide at graphite cathodes. J Phys Chem 86(14):2776–2783

45. Chang CK, Liu HY, Abdalmuhdi I (1984) Electroreduction of oxygen by pillared cobalt(II) cofacial diporphyrin catalysts. J Am Chem Soc 106(9):2725–2726

46. Shi C, Mak KW, Chan KS, Anson FC (1995) Enhancement by surfactants of the activity and stability of iridium octaethyl porphyrin as an electrocatalyst for the four-electron reduction of dioxygen. J Electroanal Chem 397(1–2):321–324

47. Collman J, Chng LL, Tyvoll DA (1995) Electrocatalytic Reduction of Dioxygen to Water by Iridium Porphyrins Adsorbed on Edge Plane Graphite Electrodes Inorg Chem 34(6):1311–1324

48. Chang CJ, Loh Z, Shi C, Anson FC, Nocera DG (2004) Targeted proton delivery in the catalyzed reduction of oxygen to water by bimetallic pacman porphyrins. J Am Chem Soc 126(32):10013–10020

49. Liu HY, Abdalmuhdi I, Chang CK et al (1985) Catalysis of the electroreduction of dioxygen and hydrogen peroxide by an anthracene-linked dimeric cobalt porphyrin. J Phys Chem 89(4):665–670

50. Collman J, Wagenknecht PS, Hutchison JE (1994) Molecular catalysts for multielectron redox reactions of small molecules—the cofacial metallodiporphyrin approach. Angew Chem Int Ed 33(15–16):1537–1554

51. Durand RR, Bencosme CS, Collman J, Anson FC (1983) Mechanistic aspects of the catalytic reduction of dioxygen by cofacial metalloporphyrins. J Am Chem Soc 105(9):2710–2718

52. Anson FC, Shi C, Steiger B (1997) Novel multinuclear catalysts for the electroreduction of dioxygen directly to water. Acc Chem Res 30(11):437–444

53. Collman J, Hendricks NH, Kim K, Bencosme CS (1987) The role of Lewis acids in promoting the electrocatalytic four-electron reduction of dioxygen. Chem Commun (20):1537

54. Ni CL, Abdalmuhdi I, Chang CK, Anson FC (1987) Behavior of four anthracene-linked dimeric metalloporphyrins as electrocatalysts for the reduction of dioxygen. J Phys Chem 91(5):1158–1166

55. Collman J, Kim K (1986) Electrocatalytic four-electron reduction of dioxygen by iridium porphyrins adsorbed on graphite. J Am Chem Soc 108(24):7847–7849

56. Bouwkamp-Wijnoltz AL, Visscher W, van Veen J (1994) Oxygen reduction catalysed by carbon supported iridium-chelates. Electrochim Acta 39(11–12):1641–1645

57. Shi C, Steiger B, Yuasa M, Anson FC (1997) Electroreduction of O_2 to H_2O at unusually positive potentials catalyzed by the simplest of the cobalt porphyrins. Inorg Chem 36(20):4294–4295

58. Zagal JH, Griveau S, Ozoemena KI, Nyokong T, Bedioui F (2009) Carbon nanotubes, phthalocyanines and porphyrins: attractive hybrid materials for electrocatalysis and electroanalysis. J Nanosci Nanotechnol 9(4):2201–2214

59. Okunola A, Kowalewska B, Bron M, Kulesza PJ, Schuhmann W (2009) Electrocatalytic reduction of oxygen at electropolymerized films of metalloporphyrins deposited onto multi-walled carbon nanotubes. Electrochim Acta 54(7):1954–1960

60. Mamuru SA, Ozoemena KI, Fukuda T, Kobayashi N (2010) Iron(II) tetrakis(diaquaplatinum) octacarboxyphthalocyanine supported on multi-walled carbon nanotube platform: an efficient functional material for enhancing electron transfer kinetics and electrocatalytic oxidation of formic acid. J Mater Chem 20(47):10705

61. Mamuru SA, Ozoemena KI (2010) Iron (II) tetrakis(diaquaplatinum) octacarboxyphthalocyanine supported on multi-walled carbon nanotubes as effective electrocatalyst for oxygen reduction reaction in alkaline medium. Electrochem Commun 12(11):1539–1542

62. Xu Z, Li H, Cao G, Zhang Q, Li K, Zhao X (2011) Electrochemical performance of carbon nanotube-supported cobalt phthalocyanine and its nitrogen-rich derivatives for oxygen reduction. J Mol Catal A: Chem 335(1–2):89–96

63. Yuan Y, Zhao B, Jeon Y, Zhong S, Zhou S, Kim S (2011) Iron phthalocyanine supported on amino-functionalized multi-walled carbon nanotube as an alternative cathodic oxygen catalyst in microbial fuel cells. Biores Technol 102(10):5849–5854

64. Morozan A, Campidelli S, Filoramo A, Jousselme B, Palacin S (2011) Catalytic activity of cobalt and iron phthalocyanines or porphyrins supported on different carbon nanotubes towards oxygen reduction reaction. Carbon 49(14):4839–4847

65. Mamuru SA, Ozoemena KI, Fukuda T, Kobayashi N, Nyokong T (2010) Studies on the heterogeneous electron transport and oxygen reduction reaction at metal (Co, Fe)

octabutylsulphonylphthalocyanines supported on multi-walled carbon nanotube modified graphite electrode. Electrochim Acta 55(22):6367–6375

66. Mamuru SA, Ozoemena KI (2010) Heterogeneous electron transfer and oxygen reduction reaction at nanostructured Iron(II) phthalocyanine and its MWCNTs nanocomposites. Electroanalysis 22(9):985–994

67. Maxakato NW, Mamuru SA, Ozoemena KI (2011) Efficient oxygen reduction reaction using ruthenium tetrakis(diaquaplatinum)octacarboxyphthalocyanine catalyst supported on MWCNT platform. Electroanalysis 23(2):325–329

68. Damos FS, Luz RC, Tanaka AA, Kubota LT (2010) Dissolved oxygen amperometric sensor based on layer-by-layer assembly using host–guest supramolecular interactions. Anal Chim Acta 664(2):144–150

69. Duarte J, Luz R, Damos F, Tanaka AA, Kubota LT (2008) A highly sensitive amperometric sensor for oxygen based on iron(II) tetrasulfonated phthalocyanine and iron(III) tetra-(N-methyl-pyridyl)-porphyrin multilayers. Anal Chim Acta 612(1):29–36

70. D'Souza F, Hsieh Y, Deviprasad GR (1998) Four-electron electrocatalytic reduction of dioxygen to water by an ion-pair cobalt porphyrin dimer adsorbed on a glassy carbon electrode. Chem Commun 9:1027–1028

71. Liu S, Xu J, Sun H, Li D-M (2000) meso-Tetrakis(4-N-benzylpyridyl)porphyrin and its supramolecular complexes formed with anionic metal–oxo cluster: spectroscopy and electrocatalytic reduction of dioxygen. Inorg Chim Acta 306(1):87–93

72. Araki K, Toma HE (2006) Supramolecular Porphyrins as Electrocatalysts. In: Zagal JH, Bedioui F, Dodelet JP (eds) N$_4$-macrocyclic metal complexes. Springer, New York, pp 255–314

73. Shi C, Anson FC (1991) Multiple intramolecular electron transfer in the catalysis of the reduction of dioxygen by cobalt meso-tetrakis(4-pyridyl)porphyrin to which four Ru(NH$_3$)$_5$ groups are coordinated. J Am Chem Soc 113(25):9564–9570

74. Shi C, Anson FC (1992) Electrocatalysis of the reduction of molecular oxygen to water by tetraruthenated cobalt meso-tetrakis(4-pyridyl)porphyrin adsorbed on graphite electrodes. Inorg Chem 31(24):5078–5083

75. Steiger B, Anson FC (1997) [5,10,15,20-tetrakis(4-((pentaammineruthenio)-cyano)phenyl) porphyrinato]cobalt(II) immobilized on graphite electrodes catalyzes the electroreduction of O$_2$ to H$_2$O, but the corresponding 4-cyano-2,6-dimethylphenyl derivative catalyzes the reduction only to H$_2$O$_2$. Inorg Chem 36(18):4138–4140

76. Shi C, Anson FC (1996) Cobalt meso- tetrakis(N-methyl-4-pyridiniumyl)porphyrin becomes a catalyst for the electroreduction of O$_2$ by four electrons when [(NH$_3$)$_5$Os]$_{n+}$ (n = 2, 3) groups are coordinated to the porphyrin ring. Inorg Chem 35(26):7928–7931

77. Zagal JH, Páez M, Sturm J, Ureta-Zanartu S (1984) Electroreduction of oxygen on mixtures of phthalocyanines co-adsorbed on a graphite electrode. J Electroanal Chem 181(1–2):295–300

78. Dobrzeniecka A, Zeradjanin A, Masa J, Stroka J, Goral M, Schuhmann W, Kulesza PJ (2011) ECS Trans 35:33–44

79. Forshey PA, Kuwana T (1983) Electrochemistry of oxygen reduction. 4. Oxygen to water conversion by iron(II)(tetrakis(N-methyl-4-pyridyl)porphyrin) via hydrogen peroxide. Inorg Chem 22(5):699–707

80. Elbaz L, Korin E, Soifer L, Bettelheim A (2008) Electrocatalytic oxygen reduction by Co(III) porphyrins incorporated in aerogel carbon electrodes. J Electroanal Chem 621(1):91–96

81. Zagal JH, Páez MA, Silva JF (2006) Fundamental Aspects on the Catalytic Activity of Metallomacrocyclics for the Electrochemical Reduction of O$_2$. In: Zagal JH, Bedioui F, Dodelet JP (eds) N$_4$-Macrocyclic Metal Complexes. Springer, New York, pp 41–82

82. Zagal JH (1992) Metallophthalocyanines as catalysts in electrochemical reactions. Coord Chem Rev 119:89–136

83. Zagal JH (2003) Macrocycles. In: Vielstich W, Lamm A, Gasteiger HA (eds) Handbook of fuel cells-fundamentals, technology and applications, vol. 2, Part 5. Wiley, Chichester

84. Tse Y, Janda P, Lam H, Zhang J, Pietro WJ, Lever ABP (1997) Monomeric and polymeric tetra-aminophthalocyanatocobalt(II) modified electrodes: electrocatalytic reduction of oxygen. J Porphyrins Phthalocyanines 1(1):3–16

85. Pavez J, Paez M, Ringuede BF, Zagal JH (2005) Effect of film thickness on the electro-reduction of molecular oxygen on electropolymerized cobalt tetra-aminophthalocyanine films. J Solid State Electrochem 9(1):21–29

86. Ramírez G, Trollund E, Isaacs M, Armijo F, Zagal JH, Costamagna J, Aguirre MJ (2002) Electroreduction of molecular oxygen on poly-iron-tetraaminophthalocyanine modified electrodes. Electroanalysis 14(7–8):540–545

87. Lalande G, Cote R, Guay D, Dodelet JP, Weng LT, Bertrand P (1997) Is nitrogen important in the formulation of Fe-based catalysts for oxygen reduction in solid polymer fuel cells? Electrochim Acta 42(9):1379–1388

88. Bouwkamp-Wijnoltz A, Visscher W, van Veen J (1998) The selectivity of oxygen reduction by pyrolysed iron porphyrin supported on carbon. Electrochim Acta 43(21–22):3141–3152

89. Lefevre M, Dodelet JP, Bertrand P (2002) Molecular oxygen reduction in PEM fuel cells: evidence for the simultaneous presence of two active sites in Fe-based catalysts. J Phys Chem B 106(34):8705–8713

90. Lefèvre M (2003) Fe-based catalysts for the reduction of oxygen in polymer electrolyte membrane fuel cell conditions: determination of the amount of peroxide released during electroreduction and its influence on the stability of the catalysts. Electrochim Acta 48(19):2749–2760

91. Schilling T, Okunola A, Masa J, Schuhmann W, Bron M (2010) Carbon nanotubes modified with electrodeposited metal porphyrins and phenanthrolines for electrocatalytic applications. Electrochim Acta 55(26):7597–7602

92. Bouwkamp-Wijnoltz AL, Visscher W, van Veen JA (2002) On active-site heterogeneity in pyrolyzed carbon-supported iron porphyrin catalysts for the electrochemical reduction of oxygen: an in situ Mossbauer study. J Phys Chem B 106(50):12993–13001

93. Kobayashi N, Nevin WA (1996) Electrocatalytic reduction of oxygen using water-soluble iron and cobalt phthalocyanines and porphyrins. Appl Organomet Chem 10(8):579–590

94. Zagal JH, Aguirre MJ, Basaez L, Pavez J, Padilla L, Toro-Labbé A (1995) Possible explanations for the volcano-shaped plots for the electrocatalytic reduction of O_2 on electrodes modified with N-4 macrocycles. In: Adzic RR, Anson FC, Kinoshita K (eds) Proceedings of the symposium on oxygen electrochemistry, 95–26. The Electrochemical Society Symposium Inc., Pennington, NJ, p 89

95. Bytheway I, Hall MB (1994) Theoretical calculations of metal-dioxygen complexes. Chem Rev 94(3):639–658

96. Wang G, Ramesh N, Hsu A, Deryn C, Rongrong C (2008) Density functional theory study of the adsorption of oxygen molecule on iron phthalocyanine and cobalt phthalocyanine. Mol Simul 34(10–15):1051–1056

97. Scherson DA, Palencsár A, Tolmachev Y, Stefan I (2008) Transition metal macrocycles as electrocatalysts for dioxygen reduction. In: Alkire RC, Kolb DM, Lipkowski J, Ross PN (eds) Electrochemical surface modification: thin films, functionalization and characterization. Wiley-VCH Verlag GmbH & Co. KGaA, Weinheim, Germany

98. Zecevic S, Simic-Glavaski B, Yeager E, Lever ABP, Minor PC (1985) Spectroscopic and electrochemical studies of transition metal tetrasulfonated phthalocyanines. Part V. Voltammetric studies of adsorbed tetrasulfonated phthalocyanines (MTsPc) in aqueous solutions. J Electroanal Chem 196(2):339–358

99. Zagal JH, Griveau S, Francisco Silva J, Nyokong T, Bedioui F (2010) Metallophthalocyanine-based molecular materials as catalysts for electrochemical reactions. Coord Chem Rev 254 (23–24):2755–2791

100. Kim S, Scherson DA (1992) In situ UV–visible reflection absorption wavelength modulation spectroscopy of species irreversibly adsorbed on electrode surfaces. Anal Chem 64(24):3091–3095

101. Stefan IC, Mo Y, Ha SY, Scherson D (2003) In situ Fe K-edge X-ray absorption fine structure of a nitrosyl adduct of iron phthalocyanine irreversibly adsorbed on a high area carbon electrode in an acidic electrolyte. Inorg Chem 42(14):4316–4321

102. Zagal JH, Bedioui F, Dodelet JP (eds) (2006) N_4-macrocyclic metal complexes. Springer, New York

103. Wiesener K, Ohms D, Neumann V, Franke R (1989) N_4 macrocycles as electrocatalysts for the cathodic reduction of oxygen. Mater Chem Phys 22(3–4):457–475

104. van Veen J (1979) Oxygen reduction on monomeric transition metal phthalocyanines in acid electrolyte. Electrochim Acta 24(9):921–928

105. van Veen JA, van Baar JF, Kroese CJ, Coolegem JGF, De Wit N, Colijn HA (1981) Oxygen reduction on transition-metal porphyrins in acid electrolyte. 1. Activity. Phys Chem Chem Phys 85(8):693–700

106. Zagal JH, Gulppi M, Isaacs M, Cárdenas-Jirón G, Aguirre MJ (1998) Linear versus volcano correlations between electrocatalytic activity and redox and electronic properties of metallophthalocyanines. Electrochim Acta 44(8–9):1349–1357

107. Appleby AJ, Zagal JH (2011) Free energy relationships in electrochemistry: a history that started in 1935. J Solid State Electrochem 15(7–8):1811–1832

108. Cardenas-Jiron GI, Gulppi MA, Caro CA et al (2001) Reactivity of electrodes modified with substituted metallophthalocyanines. Correlations with redox potentials, Hammett parameters and donor–acceptor intermolecular hardness. Electrochim Acta 46(20–21):3227–3235

109. Sehlotho N, Nyokong T (2006) Effects of ring substituents on electrocatalytic activity of manganese phthalocyanines towards the reduction of molecular oxygen. J Electroanal Chem 595(2):161–167

110. Bedioui F, Griveau S, Nyokong T, Appleby AJ, Caro CA, Gulppi M, Ochoa G, Zagal JH (2007) Tuning the redox properties of metalloporphyrin- and metallophthalocyanine-based molecular electrodes for the highest electrocatalytic in the oxidation of thiols. Phys Chem Chem Phys 9(26):3383–3396

111. Zagal JH, Ponce I, Baez D, Venegas R, Pavez J, Paez M, Gulppi M (2012) A possible interpretation for the high catalytic activity of heat-treated metal-Nx/C macrocycles for O_2 reduction in terms of formal potentials of the catalyst. Electrochem Solid-State Lett 15(6): B1–B3

112. Jaouen F, Herranz J, Lefèvre M, Dodelet JP, Kramm UI, Herrmann I, Bogdanoff P, Maruyama J, Nagaoka T, Garsuch A, Dahn JR, Olson T, Pylypenko S, Atanassov P, Ustinov EA (2009) Cross-laboratory experimental study of non-noble-metal electrocatalysts for the oxygen reduction reaction. ACS Appl Mater Interfaces 1(8):1623–1639

113. Schlettwein D, Yoshida T (1998) Electrochemical reduction of substituted cobalt phthalocyanines adsorbed on graphite. J Electroanal Chem 441(1–2):139–146

114. Zagal JH, Cárdenas-Jirón GI (2000) Reactivity of immobilized cobalt phthalocyanines for the electroreduction of molecular oxygen in terms of molecular hardness. J Electroanal Chem 489(1–2):96–100

115. Cardenas-Jiron GI, Zagal JH (2001) Donor–acceptor intermolecular hardness on charge transfer reactions of substituted cobalt phthalocyanines. J Electroanal Chem 497(1–2):55–60

116. Zagal JH, Gulppi MA, Cárdenas-Jirón G (2000) Metal-centered redox chemistry of substituted cobalt phthalocyanines adsorbed on graphite and correlations with MO calculations and Hammett parameters. Electrocatalytic reduction of a disulfide. Polyhedron 19(22–23):2255–2260

117. Newton MD (1991) Quantum chemical probes of electron-transfer kinetics: the nature of donor-acceptor interactions. Chem Rev 91(5):767–792

118. Pearson RG (1986) Absolute electronegativity and hardness correlated with molecular orbital theory. Proc Natl Acad Sci 83(22):8440–8441

119. Parr RG, Pearson RG (1983) Absolute hardness: companion parameter to absolute electro-negativity. J Am Chem Soc 105(26):7512–7516

120. Ulstrup J (1977) Catalysis of the electrochemical reduction of molecular dioxygen by metal phthalocyanines. J Electroanal Chem 79(1):191–197

121. Rosa A, Baerends EJ (1994) Metal-macrocycle interaction in phthalocyanines: density functional calculations of ground and excited states. Inorg Chem 33(3):584–595

122. Hipps KW, Lu X, Wang XD, Mazur U (1996) Metal d-orbital occupation-dependent images in the scanning tunneling microscopy of metal phthalocyanines. J Phys Chem 100(27):11207–11210

123. Jasinski R (1965) Cobalt phthalocyanine as a fuel cell cathode. J Electrochem Soc 112(5):526

124. Yeager E (1984) Electrocatalysis for O_2 reduction. Electrochim Acta 29(11):1527–1537

125. Hinnen C, Coowar F, Savy M (1989) Oxygen reduction in acid media investigations by electroreflectance on adsorbed iron phthalocyanine and naphthalocyanine layers. J Electroanal Chem 264(1–2):167–180

126. van den Ham D, Hinnen C, Magner G, Savy M (1987) Electrocatalytic oxygen reduction: the role of oxygen bridges as a structural factor in the activity of transition-metal phthalocyanines. J Phys Chem 91(18):4743–4748

127. Coowar F, Contamin O, Savy M, Scarbeck G (1988) Electrocatalysis of O_2 reduction to water in different acid media by iron naphthalocyanines. J Electroanal Chem 246(1):119–138

128. Elzing A, van der Putten A, Visscher W, Barendrecht E (1987) The cathodic reduction of oxygen at metal tetrasulfonato-phthalocyanines: influence of adsorption conditions on electrocatalysis. J Electroanal Chem 233(1–2):99–112

129. Fierro CA, Mohan M, Scherson DA (1990) *In situ* Moessbauer spectroscopy of a species irreversibly adsorbed on an electrode surface. Langmuir 6(8):1338–1342

130. Ouyang J, Shigehara K, Yamada A, Anson FC (1991) Hexadecafluoro- and octacyano phthalocyanines as electrocatalysts for the reduction of dioxygen. J Electroanal Chem 297(2):489–498

131. van der Putten A, Elzing A, Visscher W, Barendrecht E (1986) Oxygen reduction on vacuum-deposited and absorbed transition-metal phthalocyanine films. J Electroanal Chem 214(1–2):523–533

132. Song C, Zhang L, Zhang J (2006) Reversible one-electron electro-reduction of O_2 to produce a stable superoxide catalyzed by adsorbed Co(II) hexadecafluoro-phthalocyanine in aqueous alkaline solution. J Electroanal Chem 587(2):293–298

133. Kalvelage H, Mecklenburg A, Kunz U, Hoffmann U (2000) Electrochemical reduction of oxygen at pyrolyzed iron and cobalt N_4-chelates on carbon black supports. Chem Eng Technol 23(9):803–807

134. Coutanceau C, Rakotondrainibe A, Crouigneau P, Léger JM, Lamy C (1995) Spectroscopic investigations of polymer-modified electrodes containing cobalt phthalocyanine: application to the study of oxygen reduction at such electrodes. J Electroanal Chem 386(1–2):173–182

135. Elzing A, van der Putten A, Visscher W, Barendrecht E (1990) Spectroscopic measurements on metal tetrasulphonato-phthalocyanines. J Electroanal Chem 279(1–2):137–156

136. Phougat N, Vasudevan P (1997) Electrocatalytic activity of some metal phthalocyanine compounds for oxygen reduction in phosphoric acid. J Power Sources 69(1–2):161–163

137. Ponce I, Silva JF, Oñate R, Rezende MC, Páez MA, Pavez J, Zagal JH (2011) Enhanced catalytic activity of Fe phthalocyanines linked to Au(111) via conjugated self-assembled monolayers of aromatic thiols for O_2 reduction. Electrochem Commun 13(11):1182–1185

138. Sheldon RA, Kochi JK (1981) Metal-catalyzed oxidations of organic compounds. Academic, New York

139. van den Brink F, Barendrecht E, Visscher W (1980) The cathodic reduction of oxygen: A review with emphasis on macrocyclic organic metal complexes as electrocatalysts. Recl Trav Chim Pays-Bas 99:253–262

140. Elzing A, van der Putten A, Visscher W, Barendrecht E (1987) The mechanism of oxygen reduction at iron tetrasulfonato-phthalocyanine incorporated in polypyrrole. J Electroanal Chem 233(1–2):113–123

141. van den Brink F, Visscher W, Barendrecht E (1984) Electrocatalysis of cathodic oxygen reduction by metal phthalocyanines. Part III. Iron phthalocyanine as electrocatalyst: experimental part. J Electroanal Chem 172(1–2):301–325

142. Baranton S, Coutanceau C, Garnier E, Léger J-M (2006) How does α-FePc catalysts dispersed onto high specific surface carbon support work towards oxygen reduction reaction (orr)? J Electroanal Chem 590(1):100–110

143. Ikeda O, Fukuda H, Tamura H (1986) The effect of heat treatment on group VIIIB porphyrins as electrocatalysts in the cathodic reduction of oxygen. J Chem Soc Faraday Trans 1 82(5):1561

144. Anderson AB, Sidik RA (2004) Oxygen electroreduction on Fe II and Fe III coordinated to N_4 chelates. Reversible potentials for the intermediate steps from quantum theory. J Phys Chem B 108(16):5031–5035

145. Kadish KM, Smith KM, Guilard R (eds) (2003) The porphyrin handbook. Academic, San Diego, Calif, London

146. Magner G (1981) Effects of substitution of iron by molybdenum in the naphthalocyanine structures upon their electrocatalytic properties for O_2 reduction and evolution in alkaline media. J Electrochem Soc 128(8):1674

147. Baker R, Wilkinson D, Zhang J (2008) Electrocatalytic activity and stability of substituted iron phthalocyanines towards oxygen reduction evaluated at different temperatures. Electrochim Acta 53(23):6906–6919

148. Zhang L, Song C, Zhang J, Wang H, Wilkinson DP (2005) Temperature and pH dependence of oxygen reduction catalyzed by iron fluoroporphyrin adsorbed on a graphite electrode. J Electrochem Soc 152(12):A2421

149. Solomon EI, Sundaram UM, Machonkin TE (1996) Multicopper oxidases and oxygenases. Chem Rev 96(7):2563–2605

150. Mirica LM, Ottenwaelder X, Stack TD (2004) Structure and spectroscopy of copper-dioxygen complexes. Chem Rev 104(2):1013–1045

151. Schweiger H, Vayner E, Anderson AB (2005) Why is there such a small overpotential for O_2 electroreduction by copper laccase? Electrochem Solid-State Lett 8(11):A585

152. Gallaway J, Wheeldon I, Rincon R, Atanassov P, Banta S, Barton SC (2008) Oxygen-reducing enzyme cathodes produced from SLAC, a small laccase from *Streptomyces coelicolor*. Biosens Bioelectron 23(8):1229–1235

153. Vayner E, Schweiger H, Anderson AB (2007) Four-electron reduction of O_2 over multiple Cu–I centers: quantum theory. J Electroanal Chem 607(1–2):90–100

154. Sugiyama K, Aoki K (1989) Catalytic reactions of bis(1,10-phenanthroline) cuprous complex with hydrogen-peroxide at glassy-carbon and pyrolytic-graphite electrodes. J Electroanal Chem 262(1–2):211–219

155. Zagal JH, Paez C, Aguirre MJ, Garcia AM, Zamudio W (1993) Catalytic electroreduction of molecular-oxygen on Cu(II)bisdipyridyl and Cu(II)bisphenanthroline complexes adsorbed on a graphite electrode. Bol Soc Chil Quim 38(3):191–199

156. Zhang JJ, Anson FC (1993) Electrocatalysts for the reduction of O_2 and H_2O_2 based on complexes of Cu(II) with the strongly adsorbing 2,9-dimethyl-1,10-phenanthroline ligand. Electrochim Acta 38(16):2423–2429

157. Zhang JJ, Anson FC (1993) Complexes of Cu(II) with electroactive chelating ligands adsorbed on graphite-electrodes - Surface coordination chemistry and electrocatalysis. J Electroanal Chem 348(1–2):81–97

158. Lei YB, Anson FC (1994) Mechanistic aspects of the electroreduction of as catalyzed by copper-phenanthroline complexes adsorbed on graphite-electrodes. Inorg Chem 33(22):5003–5009

159. Lei YB, Anson FC (1995) Dynamics of the Coordination equilibria in solutions containing copper(II), copper(I), and 2,9-dimethyl-1,10-phenanthroline and their effect on the reduction of O_2 by Cu(I). Inorg Chem 34(5):1083–1089

160. Marques AL, Zhang JJ, Lever AB (1995) Poisoning effect of SCN⁻, H$_2$S and HCN on the reduction of O$_2$ and H$_2$O$_2$ catalyzed by a 1:1 surface complex of Cu-1,10-phenanthroline adsorbed on graphite electrodes, and its possible application in chemical analysis. J Electroanal Chem 392(1–2):43–53

161. Losada J, del Peso I, Beyer L (2001) Electrochemical and spectroelectrochemical properties of copper(II) Schiff-base complexes. Inorg Chim Acta 321(1–2):107–115

162. Dias VL, Fernandes EN, da Silva LSM, Marques EP, Zhang J, Marques ALB (2005) Electrochemical reduction of oxygen and hydrogen peroxide catalyzed by a surface copper (II)-2,4,6-tris(2-piridil)-1,3,5-triazine complex adsorbed on a graphite electrode. J Power Sources 142(1–2):10–17

163. Weng YC, Fan FR, Bard AJ (2005) Combinatorial biomimetics. Optimization of a composition of copper(II) poly-L-histidine complex as an electrocatalyst for O$_2$ reduction by scanning electrochemical microscopy. J Am Chem Soc 127(50):17576–17577

164. Wang M, Xu X, Gao J, Jia N, Cheng Y (2006) Electrocatalytic reduction O$_2$ at pyrolytic graphite electrode modified by a novel copper(II) complex with 2-[bis(2-aminoethyl)amino] ethanol and imidazole ligands. Russ J Electrochem 42(8):878–881

165. Pichon C, Mialane P, Dolbecq A, Marrot J, Riviere E, Keita B, Nadjo SF (2007) Characterization and electrochemical properties of molecular icosanuclear and bidimensional hexanuclear Cu(II) azido polyoxometalates. Inorg Chem 46(13):5292–5301

166. Hermann A, Silva LS, Peixoto CRM, Oliveira ABD, Bordinhão J, Hörner M (2008) Electrochemical properties of Cu$_4$[PhN$_3$C$_6$H$_4$N$_3$(H)Ph]$_4$(μ-O)$_2$, a tetranuclear Copper(II) complex with 1-phenyltriazenido-2-phenyltriazene-benzene as ligand. Eclet Quím 33(3):43–46

167. Thorum MS, Yadav J, Gewirth AA (2009) Oxygen reduction activity of a copper complex of 3,5-diamino-1,2,4-triazole supported on carbon black. Angew Chem Int Ed 48(1):165–167

168. McCrory CCL, Ottenwaelder X, Stack TDP, Chidsey CED (2007) Kinetic and mechanistic studies of the electrocatalytic reduction of O$_2$ to H$_2$O with mononuclear Cu complexes of substituted 1,10-phenanthrolines. J Phys Chem A 111(49):12641–12650

169. McCrory CCL, Devadoss A, Ottenwaelder X, Lowe RD, Stack TDP, Chidsey CED (2011) Electrocatalytic O$_2$ reduction by covalently immobilized mononuclear copper(I) complexes: evidence for a binuclear Cu$_2$O$_2$ intermediate. J Am Chem Soc 133(11):3696–3699

170. Zhang JJ, Anson FC (1992) Electrochemistry of the Cu(II) complex of 4,7-diphenyl-1,10-phenanthrolinedisulfonate adsorbed on graphite electrodes and its behavior as an electrocatalyst for the reduction of O$_2$ and H$_2$O$_2$. J Electroanal Chem 341(1–2):323–341

171. Masa J, Ozoemena K, Schuhmann ZJH (2012) Oxygen reduction reaction using N$_4$-metallomacrocyclic catalysts: fundamentals on rational catalyst design. J Porphyrins Phthalocyanines 16(7):761

172. Barton SC, Kim H, Binyamin G, Zhang Y, Heller A (2001) The "Wired" laccase cathode: high current density electroreduction of O2 to water at +0.7 V (NHE) at pH 5. J Am Chem Soc 123(24):5802–5803

173. Barton SC, Kim H, Binyamin G, Zhang Y, Heller A (2001) Electroreduction of O$_2$ to water on the "Wired" Laccase Cathode †. J Phys Chem B 105(47):11917–11921

174. Soukharev V, Mano N, Heller A (2004) A four-electron O$_2$-electroreduction biocatalyst superior to platinum and a biofuel cell operating at 0.88 V. J Am Chem Soc 126(27):8368–8369

175. Ralph TR, Hogarth MP (2002) Catalysis for low temperature fuel cells Part I: The cathode challenges. Platinum Metals Rev 46(1):3–14

176. Hu X, Liu C, Wu Y, Zhang Z (2011) Structure–reactivity relationships of metalloporphyrin modified by ionic liquid and its analogue. J Phys Chem C 115(48):23913–23921

177. Masa J, Schilling T, Bron M, Schuhmann W (2011) Electrochemical synthesis of metal–polypyrrole composites and their activation for electrocatalytic reduction of oxygen by thermal treatment. Electrochim Acta 60:410–418

1723 178. Xia W, Masa J, Bron M, Schuhmann W, Muhler M (2011) Highly active metal-free nitrogen-
1724   containing carbon catalysts for oxygen reduction synthesized by thermal treatment of
1725   polypyridine-carbon black mixtures. Electrochem Commun 13(6):593–596
1726 179. Masa J, Bordoloi A, Muhler M, Schuhmann W, Xia W (2012) Enhanced electrocatalytic
1727   stability of platinum nanoparticles supported on a nitrogen-doped composite of carbon
1728   nanotubes and mesoporous titania under oxygen reduction conditions. ChemSusChem
1729   5:523–525
1730 180. Mittasch A, Frankenburg W (1950) Early studies of multicomponent catalysts. Adv Catal
1731   2:81–104
1732 181. Dembinska B, Kulesza PJ (2009) Multi-walled carbon nanotube-supported tungsten oxide-
1733   containing multifunctional hybrid electrocatalytic system for oxygen reduction in acid
1734   medium. Electrochim Acta 54(20):4682–4687
1735 182. Baranton S, Coutanceau C, Roux C et al (2005) Oxygen reduction reaction in acid medium at
1736   iron phthalocyanine dispersed on high surface area carbon substrate: tolerance to methanol,
1737   stability and kinetics. J Electroanal Chem 577(2):223–234
1738 183. Lu Y, Reddy R (2007) The electrochemical behavior of cobalt phthalocyanine/platinum as
1739   methanol-resistant oxygen-reduction electrocatalysts for DMFC. Electrochim Acta
1740   52(7):2562–2569

Author Queries

Chapter No.: 7

Query Refs.	Details Required	Author's response
AU1	Please provide affiliation details for the authors Justus Masa, Kenneth Ozoemena, Wolfgang Schuhmann	
AU2	Please provide closing parenthesis for "([Co(TMPyP]$^{4+}$ Cl$_4^-$)".	
AU3	Please provide opening square bracket for "meso-tetrakis(4-sulfonatophenyl) porphyrinato]cobalt".	
AU4	Please provide closing square bracket for "([(Na$^+$)$_4$[Co(TPPS)]$^{4-}$)".	
AU5	Please note that part figure label (a) mentioned in the caption of the Fig. 7.14 has been deleted.	
AU6	Please check the insertion of list number (1) is appropriate in the sentence "The first step…"	
AU7	Please check the insertion of parenthesis in caption of Fig. 7.15	
AU8	Please check the term "x.Co-Co" for correctness.	
AU9	The author group "Chen et al." given in the sentence "In the case of the side-on interaction…" does not match with Ref. [96]. Please check	
AU10	Please check if edit to the sentence starting "The latter…." is okay.	
AU11	Please check if edit to the sentence starting "The catalysts…." is okay.	
AU12	Please provide closing parenthesis for "Co(III/(II)".	
AU13	Please provide the volume number for Ref. [54]	